Low-dose interleukin-2 reverses behavioral sensitization in multiple mouse models of headache disorders

Jintao Zhang[1,2,5], **Katherine Czerpaniak**[1,2], **Liang Huang**[1,2,6], **Xuemei Liu**[1,2], **Megan E Cloud**[1,2], **Jacqueline Unsinger**[1], **Richard S Hotchkiss**[1,3,4], **Daizong Li**[1,2], **Yu-Qing Cao**[1,2,*]

[1]Department of Anesthesiology, Washington University School of Medicine, St. Louis, MO 63110;

[2]Washington University Pain Center, Washington University School of Medicine, St. Louis, MO 63110;

[3]Department of Medicine, Washington University School of Medicine, St. Louis, MO 63110;

[4]Department of Surgery, Washington University School of Medicine, St. Louis, MO 63110;

[5]Department of Anesthesiology, Nanfang Hospital, Southern Medical University, Guangzhou, China 510510

[6]Present address: Department of Anesthesiology, New York University Langone Health, New York University Grossman School of Medicine, New York, NY 10016

1. Introduction

Headache disorders, including chronic migraine, post-traumatic headache (PTH) and medication overuse headache (MOH), are highly prevalent and debilitating [20,40,57]. A substantial proportion of patients remain either unresponsive to current treatment options or intolerant to their side effects. There is an urgent need to understand the disease mechanisms and to develop safer and more effective therapies with mechanisms of action distinct from the existing approaches.

Activation of many pro-inflammatory immune cells, including meningeal mast cells, macrophages, dendritic cells and T cells, have been implicated in the pathophysiology of migraine and PTH [9,37,41,48,51]. On the contrary, little is known about the involvement of immunosuppressive regulatory T (Treg) cells in headache disorders, let alone their potential as a therapeutic target. Tregs are a specialized subpopulation of CD4$^+$ T cells that express high-level of transcription factor Foxp3 and the high-affinity interleukin-2 (IL2) receptor CD25 [52]. They possess far-ranging suppressive activity affecting the function of all types of immune cells with multiple mechanisms, therefore are widely implicated in the maintenance of immune homeostasis [52]. Many clinical trials use repeated low-dose interleukin-2 (ld-IL2) treatment to selectively expand and activate Treg cells *in vivo* without

---

*Corresponding author: Yu-Qing Cao, Department of Anesthesiology and Pain Center, Washington University School of Medicine, 660 South Euclid, Box 8054, St. Louis, MO 63110, Tel: +1-314-362-8726, Fax: +1-314-362-8334, caoy@anest.wustl.edu.

The authors report no conflict of interests.

activating effector T cells regardless of the disease background [30,49]. Ld-IL2 is well tolerated in patients and show indications of clinical efficacy [49,54].

Chronic pain-associated Treg changes have been studied in mouse models of nerve injury and experimental autoimmune encephalomyelitis (EAE). Nerve injury reduces Treg cells in mouse spleen [25] but increases Treg cell number in the injured nerve as well as the ipsilateral draining lymph node (LN), dorsal root ganglia (DRG) and dorsal horn of the spinal cord [36]. EAE also results in Treg increases in the brain, spinal cord, LN and spleen [21]. In both disease models, cutaneous mechanical allodynia is exacerbated by the depletion of Treg cells and is attenuated by the increase in Treg cell number [4,21,25,36,38].

In this study, we conducted the first preclinical study to test the hypothesis that ld-IL2 treatment may prevent and/or reverse the chronification of migraine and other headache disorders. Repeated injections of nitroglycerin (NTG, a nitric oxide [NO] donor and a reliable trigger of migraine in patients) resulted in a 50% reduction of the ratio of Treg cells among $CD3^+$ T cells in mouse trigeminal ganglia (TG), suggesting that chronic migraine is associated with a deficiency in Treg-mediated immune homeostasis. Ld-IL2 treatment not only completely reversed NTG-induced facial skin hyper-sensitivity, but also blocked the effects of subsequent NTG administrations through endogenous Treg cells. Importantly, ld-IL2 did not alter basal nociceptive responses or induce the development of tolerance. Ld-IL2 also effectively reversed the behavioral sensitization related to MOH, and prevented the development of both acute and persistent PTH-related behaviors in a mouse model of mild traumatic brain injury (mTBI). Collectively, the present study identifies Treg cell as a promising target for treating chronic migraine. Our results support the potential of ld-IL2 as a safe and effective treatment for multiple headache disorders with a mechanism of action distinct from the existing treatment approaches.

2. Materials and Methods

2.1. Mice

All procedures were carried out in strict accordance with the recommendations in the Guide for the Care and Use of Laboratory Animals of the National Institutes of Health and were approved by the Institutional Animal Care and Use Committee at Washington University in St. Louis. To avoid social isolation stress, all mice were group housed (2–5 per cage, same sex) in the animal facility of Washington University in St. Louis on a 12-hour light–dark cycle with constant temperature (23–24°C), humidity (45–50%), and food and water *ad libitum*. All experiments were performed during the light phase (9 am to 4 pm). Adult mice (8–14 weeks old, both male and female) were used in the experiments. Adult Swiss Webster mice were purchased from Charles River. Adult C57BL/6J mice and the breeders of DEREG (depletion of regulatory T cell, 32050-JAX) mice were purchased from the Jackson Laboratory. The DEREG mice contain a transgenic allele that expresses the diphtheria toxin receptor-enhanced green fluorescent protein (DTR-EGFP) fusion protein under the control of the genomic sequences that regulate the expression of endogenous *foxp3* [35]. Heterozygous DEREG mice were generated by crossing the DEREG breeder with C57BL6/J mice. The genotype was determined by polymerase chain reaction of tail DNA. The DTR-EGFP transgenic allele was amplified with the forward primer (5'-

CCTACGGCGTGCAGTGCTTCAGCCGC-3') and the reverse primer (5'-CGGCGAGCTGCACGCTGCCGTCCTC-3'), producing a 300-bp fragment. The PCR conditions were 96°C for 30 seconds (s), 60°C for 30 s and 72°C for 30 s for 33 cycles. Of note, DEREG mice were used as a reporter line for Foxp3^{+} Treg cells, not for depletion of Treg cells in this study.

2.2. Mouse models of headache disorders

2.2.1. Mouse model of chronic migraine and drug treatments—After measuring baseline nociceptive responses, mice received repetitive intraperitoneal (i.p.) injections of NTG (10 mg/kg in saline with 1% propylene glycol) or vehicle (saline with 1% propylene glycol in saline, 10 ml/kg) every 2 days for 4 or more times as described previously [47]. Nocifensive behaviors were measured two days after each injection (before the next treatment). NTG (Copperhead Chemical, SDM27) was freshly diluted from the stock (10% in propylene glycol, aliquoted in airtight glass vials and stored at 4°C) with saline for every injection.

Recombinant mouse IL2 (Biolegend, carrier-free) was freshly diluted from the stock (1 mg/ml aliquots at −80°C) every day. Each mouse received daily i.p. injection of 1 μg IL2 in 100 μl saline. The control mice received daily i.p. injections of 100 μl saline. In Treg depletion experiment, mice received 1 i.p. injection of antibodies against CD25 (500 μg/mouse, BioXcell, BP0012, [11]) or control IgG ((BioXcell, BP0088). The antibody binds to CD25 on Treg cell membrane and deplete Treg cells through Fcγ receptor III-mediated antibody-dependent-cellular-cytotoxicity and antibody-dependent-cellular-phagocytosis [53]. Note that on the days that the mouse behaviors were tested, NTG, IL2 and/or antibodies were always injected after completing the behavioral tests.

2.2.2. Mouse model of mild traumatic brain injury (mTBI)-induced PTH—Adult Swiss Webster mice (30–35 g) were subjected to mTBI using a modified closed head weight-drop method [43,58]. Briefly, mice were anesthetized with 3% isoflurane for 90 seconds and were placed chest down on a foam sponge (4 cm thickness, 0.062 g/cm^3 density) directly underneath a hollow cylindrical tube (1.5 cm inner diameter) placed approximately 1 cm vertically over the mouse's head. To induce mTBI, a 30 g weight (1.3 cm diameter, 3.4 cm height) was dropped through the tube from a height of 80 cm, striking the center point between the ears once. All mice regained righting reflex within 2 minutes. No mortality, skull fracture or motor deficit was observed in any mice. Sham mice were anesthetized with 3% isoflurane for 90 seconds but not subjected to the weight drop. Facial mechanical thresholds were measured before and at various time points after mTBI. Daily ld-IL2 or saline were administered 1 or 7 days after the sham or mTBI procedure. To reveal mTBI-induced hyperalgesia priming, mice received daily i.p. injections of NTG (0.1 mg/kg i.p.) for 4 to 6 days, starting at 35 days post-mTBI. Facial mechanical thresholds were measured between day 35 and 43 post-mTBI. Note that on the days that the mouse behaviors were tested, NTG and/or IL2 were always injected after completing the behavioral tests.

2.2.3. Mouse model of MOH—After measuring baseline nociceptive responses, mice received daily i.p. injections of sumatriptan succinate (Fresenius Kabi, 0.6 mg/kg, [44]).

Daily ld-IL2 or saline were administered after mice received 2 sumatriptan injections. Facial and hindpaw mechanical thresholds were measured every two days. Note that on the days that the mouse behaviors were tested, sumatriptan and/or IL2 were always injected after completing the behavioral tests.

2.3. Behavioral Tests

Mice were extensively handled by the experimenters for 2 weeks and were well-habituated to the test room and the test apparatus before each experiment. The experimenters were blinded to the treatments mice received during data collection and analysis.

2.3.1. Open field test—Mice were habituated in the testing room for 1 hour in their home cages and then tested one at a time. Each mouse was placed in the center of the dimly illuminated, sound-attenuated VersaMax Open Field box (42×42 cm, AccuScan Instruments) for 1 hour while the experimenter left the room. Horizontal movement and center entries (14×14 cm) were recorded and analyzed by the VersaMax software.

2.3.2. Rotarod test—Motor coordination was assessed with the rotarod test 6 days post-mTBI. Male mice were habituated in the testing room for 1 hour in their home cages and then underwent 5 training sessions on the Rotarod (Ugo Basile, Model 7650) at 4 revolutions/min (rpm) for 5 minutes. Mice that stayed on the rod for at least 2 minutes/session were tested on the accelerating rod (4 to 40 rpm over 5.5 minutes). The latency to fall from the rod was averaged over 3 trials in individual mice.

2.3.3. Adhesive removal test—We used the adhesive removal test to assess mTBI-induced sensory and motor deficits related to the paw and the mouth [7]. The mouse was habituated in a testing box ($28.5 \times 17.5 \times 12$ cm) for 60 s. Two pieces of adhesive tape strips (0.3 cm $\times 0.4$ cm, Topcare) were applied with equal pressure on each forepaw to cover the glabrous skin. Tape removal time was defined as the time between the mouse's first reaction to the presence of the tape, either by shaking its paw or bringing its paw to its mouth, and the complete removal of the adhesive strip from the forepaw. Male mice underwent 3 training sessions on post-mTBI day 11 and 2 test sessions the next day. The tape removal times of the left and right forepaws from the two test sessions were averaged in individual mice.

2.3.4. Responses to mechanical stimuli on the hindpaw—Mice were habituated in individual clear plexiglass boxes ($11 \times 11 \times 15$ cm) for 1–2 hours. A series of calibrated von Frey filaments was used to apply mechanical stimuli to the plantar surface of the hindpaws. We used the up-down paradigm to determine the 50% withdrawal threshold [12]. The thresholds for both hindpaws were averaged to yield a single value for each mouse.

2.3.5. Cheek acetone test—The acute nocifensive response to acetone-evoked evaporative cooling on mouse cheek was measured as previously described [14]. The day before testing, both cheeks were shaved (6.5×12 mm) under brief anesthesia (2% isoflurane in 100% oxygen). On the test day, mice were habituated in individual plexiglass cylinders (11 cm diameter, 15 cm height) situated in front of 3-way mirrors for 1–2 hours. We applied

acetone (12 μl) to the shaved cheeks and immediately returned mice to the cylinders. Time spent wiping the treated area was recorded by a video camera and quantified off-line. For individual mice, acetone was applied alternatingly to both cheeks at > 10-minute intervals, and the duration of behavior was averaged from 4 applications.

2.3.6.   Withdrawal responses to facial mechanical stimuli—The hair on mouse forehead (above and between two eyes) was shaved the day before testing. On the test day, the experimenter gently held the mouse on the palm with minimal restraint and applied the calibrated von Frey filament perpendicularly to the shaved skin, causing the filament to bend for 5 seconds. A positive response was determined by the following criteria as previously described: mouse vigorously stroked its face with the forepaw, head withdrawal from the stimulus, or head shaking [22]. The up-down paradigm was used to determine the 50% withdrawal threshold [12].

2.4.   Blood, spleen and cervical LN cell preparation, antibody staining, flow cytometry and ELISA (enzyme-linked immunosorbent assay)

Adult male DEREG and C57BL6/J mice received 15 daily injections of saline or IL2. About 100 μl blood was collected from each mouse by submandibular bleeding. Mice used for blood collection were not used in the behavioral tests. Spleen and cervical LN tissues were ground and filtered through a sterile 70-μm cell strainer. After lysis of red blood cells (Biolegend, 420301), cells were pelleted and resuspended for antibody staining, ELISA and ELISPOT assay. Live cells were counted by the Vi-CELL Automated Cell Viability Analyzer (Beckman).

About 2×10^6 suspension cells were stained with the following antibodies from Biolegend that recognize mouse CD3ε (clone 145–2C11), CD4 (clone GK1.5 and RM4–5), CD8 (clone 53–6.7) and CD25 (clone PC61). The percentages of individual cell phenotypes were determined via flow cytometric analysis. Data were collected with FACScan (Becton Dickinson) and analyzed with CellQuest Pro (Becton Dickinson) and Rainbow X Alias (Cytek) softwares. Table 1 summarizes the markers and assays used to define T cell subsets in this study.

To quantify interferon γ (IFNγ) secretion, splenocytes were plated in 24-well plates (5×10^6 per well) and stimulated with anti-CD3 and anti-CD28 antibodies (1 μg/ml and 5μg/ml) in 1 ml complete RPMI1640 media overnight. IFNγ in the supernatants were quantified by ELISA (Biolegend, 430901).

ELISPOT assay was performed to determine the number of INFγ-secreting cells. Splenocytes were plated at 5×10^4 cells per well and incubated overnight with RPMI1640 media containing anti-CD3 and anti-CD28 antibodies (500 ng/ml and 5 μg/ml) for stimulation. IFNγ was detected using a colorimetric reagent kit (R&D SEL485 and SEL002). Following development, images were captured and analyzed on the ImmunoSpot7.0 plate reader (Cellular Technologies).

2.5. Isolation and adoptive transfer of Treg cells and CD25⁻CD4⁺ T cells

Adult C57BL/6J mice (8–12 weeks old) received daily injections of IL2 for 12 days. $CD25^+CD4^+$ Treg cells and $CD25^-CD4^+$ cells were isolated from splenocytes through $CD4^+$ T cell negative selection followed by a $CD25^+$ T cell positive selection using EasySep mouse $CD4^+$ T cell pre-enrichment and CD25 positive selection kits (Stem Cell Technologies, 18783).

Adult male C57BL/6J mice (8–14 weeks old) received i.p. injections of 10 mg/kg NTG every 2 days. One day after the 2nd NTG injection, mice were injected with 1×10^6 Treg or $CD25^-CD4^+$ cells via the tail vein. The 50% withdrawal threshold to facial mechanical stimuli was measured before the 1st NTG injection and 2 days after each NTG injections.

2.6. Tissue preparation, immunohistochemistry, and image analysis

Mice were euthanized with i.p. injection of barbiturate (200 mg/kg) and were transcardially perfused with warm 0.1 M phosphate-buffered saline (pH 7.2) followed by cold 4% formaldehyde in 0.1 M phosphate buffer (pH 7.2) for fixation. TG, lumbar L4 DRG and the tissues containing the cervical/medullary dorsal horn (from obex to C3 cervical spinal cord) were collected and sectioned at 15 μm in the transverse plane, collected on Superfrost Plus glass slides in sequence and stored at −20°C.

One in every 4 TG, DRG or cervical/medullary dorsal horn sections were processed for each immunohistochemistry experiment as described previously [27]. The dura was carefully dissected from the skull using forceps and stained as whole-mount. T cells were identified by the rat anti-CD3 antibody (eBioscience, clone 17A2, 1:200) and Treg cells were identified with the chicken anti-EGFP (AVES Lab, 1:1000) antibody in tissues from DEREG mice. AlexaFluor 568- or 488-conjugated secondary antibodies (Invitrogen) were used at 1:1000 dilution. Immunofluorescence was observed through a 40x objective on a Nikon TE2000S inverted epifluorescence microscope and images were captured with a CoolSnapHQ2 camera (Photometrics). To quantify $CD3^+$ T cells and Treg cells on the dura, we took random, non-overlapping images (10 per mouse) in areas adjacent to the middle meningeal artery (MMA). To quantify T cells and Treg cells in TG, DRG and cervical/ medullary dorsal horn, all cells on individual sections were counted, and the number was multiplied by 4 to obtain the total number of cells per ganglion in each mouse. Images of individual sections were captured by an Olympus NanoZoomer Whole-Slide Imaging System and measured with the SimplePCI software (Hamamatsu) to verify that the total areas of the sections quantified were comparable between individual mice. Representative images were adjusted for contrast and brightness using the same parameter within individual experiments. No other manipulations were made to the images. Image analysis was done with experimenters blinded to the experimental groups.

2.7. Statistical analysis

For behavioral experiments, power analysis was conducted to estimate sample size with > 80% power to reach a significance level of 0.05. The experimenters were blinded to the treatments mice received. For flow cytometry, ELISA and immunohistochemistry experiments, sample sizes were estimated based on our prior experience.

All data are reported as mean ± standard error of the mean. The Shapiro–Wilk test was used to check data normality. Statistical significance between experimental groups with normally distributed data was assessed by two-tailed t-test, ANOVA (1-way or 2-way, with or without repeated-measures [RM]) with the post hoc Bonferroni test where appropriate, using Origin and Statistica softwares (from OriginLab and StatSoft, respectively). The non-parametric Mann–Whitney U test, Friedman test or Kruskal-Wallis ANOVA on ranks with multiple comparisons (Student-Newman-Keuls method) was used to analyze the differences in the withdrawal threshold to mechanical stimuli. Differences with $p < 0.05$ were considered statistically significant. The statistical analysis for individual experiments was described in figure legends.

3. Results

3.1. Repeated NTG treatment reduces the ratio of Treg cells to total T cells in mouse TG.

To mimic the high frequency recurring headache in chronic migraine patients, we treated male and female C57BL/6J inbred mice with NTG (10 mg/kg, i.p.) or vehicle every two days for 5 times and measured the 50% withdrawal thresholds to von Frey filaments on the hindpaws two days after each injection (Fig. 1A). Compared with the baseline thresholds, repetitive NTG injections induced a progressive and sustained mechanical hyper-sensitivity on the hindpaw of both male and female mice (Fig. 1B), consistent with the previous study [24,47]. Two days after the last NTG or vehicle injection, we stained the whole-mount dura as well as the TG and L4 DRG sections with the CD3 antibody to label all T cells. The density of CD3$^+$ T cells in the dura surrounding the MMA or in L4 DRG was not altered by the repeated NTG treatment (Fig. 1C–D). In contrast, the abundance of CD3$^+$ cells was nearly doubled in the TG of NTG-treated mice (Fig. 1D–E). There were on average 2176 ± 288 and 4135 ± 562 CD3$^+$ cells per TG from vehicle- and NTG-treated mice (n =6/group, same mice as in Fig. 1D), indicating that repeated NTG administration preferentially increases the density of total T cells in mouse TG.

Next, we asked whether repeated NTG treatment alters the number of Treg cells in mouse TG, using the DEREG transgenic mice which specifically express the DTR-EGFP fusion protein in Treg cells [35]. Flow cytometric analysis showed that EGFP signal was present in 85 ± 2% CD4$^+$CD25$^+$ splenocytes from adult DEREG mice (n = 4). We verified that NTG-induced hindpaw mechanical hyper-sensitivity was not affected by the expression of DTR-EGFP in DEREG mice (Fig. 1F inset). The total number of EGFP$^+$ Treg cells was very low in TG and DRG from vehicle-treated mice (~30 and 6 per ganglion, respectively), and neither was significantly altered by the repetitive NTG injections (Fig. 1F). Since TG from NTG-treated mice contained twice as many CD3$^+$ cells than those from vehicle-treated mice, the proportion of Treg cells among total T cells in TG was significantly reduced by the repeated NTG administration. We speculate that chronic migraine is associated with a deficiency in Treg-mediated immune homeostasis.

3.2. Daily ld-IL2 prevents the development of NTG-induced skin hyper-sensitivity.

It is well documented that ld-IL2 treatment selectively expands and activates Treg cells in both mice and humans [30,32,50]. We treated male DEREG mice with daily ld-IL2 (1 μg/

mouse, i.p., [56]) or saline for 15 days. The frequency of EGFP^{+} Treg cells in the peripheral blood increased by more than 100% after 5 ld-IL2 injections (Fig. 2A), similar to the magnitude of ld-IL2-induced Treg expansion reported in human clinical trials [26,49]. The abundance of Treg cells in the blood was maintained by the subsequent IL2 injections (Fig. 2A). The percentage of EGFP^{+} Treg cells also increased significantly in the cervical LNs that receive all of the lymph from the head and neck (Fig. 2B). We also used CD25 as the marker for Treg cells and saw similar ld-IL2-induced increase in the blood and LN (Fig. 2C–D). Conversely, the frequencies of CD4^{+} and CD3^{+} T cells in the blood or LNs were not altered by the ld-IL2 treatment (Fig. 2E–F, Table 1). In wild-type C57BL6 males, 15 days of ld-IL2 treatment doubled the number and the frequency of CD25^{+}CD4^{+} Treg cells in the spleen (Fig. 3A–C), whereas the number of CD8^{+} cells increased only slightly (Fig. 3D–E). The number of splenocytes secreting IFNγ was not altered but the amount of CD3/CD28 stimulation-induced IFNγ secretion was significantly reduced in cells from IL-2 treated mice (Fig. 3F–G, Table 1). These data confirmed that daily ld-IL2 treatment preferentially increases Treg cells in the blood, LNs and spleen, enhancing immunosuppression in mice.

We proceeded to treat male C57BL/6J mice with daily saline or ld-IL2, starting 5 days before the first NTG injection and continuing throughout the experiment (Fig. 4A). Basal hindpaw mechanical sensitivity was not altered by either 5 or 15 days of ld-IL2 injections (Fig. 4B, vehicle+saline versus vehicle+IL2). Conversely, NTG-induced hindpaw mechanical hyper-sensitivity was completely blocked by the ld-IL2 pretreatment (Fig. 4B, NTG+saline versus NTG+IL2).

In addition to increasing hindpaw mechanical sensitivity, repeated NTG administration also enhances the behavioral responses to acetone-induced cooling of facial skin in mice [29], and this can be blocked by the daily treatment with topiramate, a migraine preventive drug in humans (Cloud and Cao, manuscript in preparation). After measuring baseline responses to acetone-induced cooling, we repeatedly injected female C57BL/6J mice with NTG and measured the duration of acetone-induced face wiping two days after each injection (Fig. 4A). Compared with the vehicle group, there was a persistent increase in the duration of acetone-induced cheek wiping in NTG-treated mice (Fig. 4C, vehicle+saline versus NTG +saline). Pretreatment with ld-IL2 did not change the basal responses to acetone-induced cooling (Fig. 4C, vehicle+saline versus vehicle+IL2), but prevented the development of NTG-induced facial cold hyper-sensitivity (Fig. 4C, NTG+saline versus NTG+IL2). We conclude that ld-IL2 pretreatment can effectively prevent the development of repetitive NTG-induced skin hyper-sensitivity without compromising the baseline responses to mechanical or cold stimuli.

As in C57BL/6J females, repetitive NTG induced a gradual increase in the duration of acetone-induced cheek wiping in the outbred female Swiss Webster mice (Fig. 4D). Here, we started daily ld-IL2 treatment after mice received two NTG injections but before the facial cold hyper-sensitivity was fully established (Fig. 4D). The delayed ld-IL2 treatment also blocked the development of facial cold hyper-sensitivity (Fig. 4D).

Does ld-IL2 increase the number of Treg cells in dura and TG? After 15 days of ld-IL2 treatment, there was a 4-fold increase in the density of EGFP^{+} Treg cells in the dura

surrounding the MMA in male DEREG mice (Fig. 5A–B), whereas the density of $CD3^+$ T cells was not altered (~ 80 cells/mm^2, similar to those of Fig. 1C). Consequently, ld-IL2 increased the frequency of Treg cells among $CD3^+$ cells from 5% to 20% (Fig. 5C). The number of $EGFP^+$ Treg cells increased 9-fold in the TG after ld-IL2 (Fig. 5D–E), much higher than NTG-induced 2-fold increase in total $CD3^+$ cells (Fig. 1D). Ld-IL2 treatment also resulted in a 4-fold increase in the number of $EGFP^+$ Treg cells in DRG (Fig. 5F). These data suggest that ld-IL2 pretreatment inhibits chronic migraine-related behaviors through increasing the proportion of Treg cells among total T cells in dura, TG and DRG.

3.3. NTG-induced persistent skin hyper-sensitivity is completely reversed by ld-IL2 treatment.

We went on to test whether ld-IL2 can reverse the established facial skin hyper-sensitivity resulting from repeated exposure to NTG in mice. Previous studies indicate that repeated enhancing of NO signaling results in a persistent facial mechanical hyper-sensitivity that can be blocked by the migraine preventive drug propranolol [6,15]. In female Swiss Webster mice, the mechanical threshold at the periorbital region was already substantially reduced 2 days after the first NTG injection (Fig. 6A, NTG+saline group, day 1 versus day 3). The facial mechanical hyper-sensitivity was sustained during the subsequent NTG injections (Fig. 6A, NTG+saline group, day 3–13). We started ld-IL2 treatment after mice received two NTG injections (Fig. 6A). Baseline facial mechanical threshold was not altered by daily ld-IL2 (Fig. 6A, vehicle+saline versus vehicle+IL2). Conversely, NTG-induced mechanical hyper-sensitivity started to reverse after 5 days of ld-IL2 treatment (Fig. 6A, day 9, NTG +saline versus NTG+IL2). After 7–9 days of IL2 injections, the facial mechanical threshold of mice in the NTG+IL2 group was not different from those in the vehicle+saline or vehicle +IL2 groups (Fig. 6A, day 11–13), indicating that ld-IL2 can completely reverse the established persistent facial mechanical hyper-sensitivity resulting from repeated NTG injections.

We repeated the experiment in female C57BL6/J mice. The development and maintenance of NTG-induced sensitization was similar to that seen in Swiss Webster females (Fig. 6B, NTG+saline group), and 3 injections of ld-IL2 was sufficient to completely reverse the effect of repeated NTG (Fig. 6B, NTG+IL2 group). Moreover, continuous ld-IL2 treatment prevented subsequent NTG administrations from inducing behavioral sensitization (Fig. 6B, day 7–11). We also tested whether ld-IL2 and/or Treg transfer blocks NTG-induced acute reduction of facial mechanical threshold, which models the sensory hyper-sensitivity during a migraine episode in humans ([19,23,31,39]). The facial mechanical threshold of naïve C57BL/6J mice was significantly reduced 3 hours after systemic injection of NTG (10 mg/kg i.p., Fig. 6C day 1). After NTG-induced persistent facial skin hyper-sensitivity was completely reversed by ld-IL2 (day 11 in Fig. 6B), a subsequent NTG injection did not cause an acute reduction of facial mechanical threshold 3 hours later (Fig. 6C day 11), suggesting that ld-IL2 prevents the onset of migraine episodes triggered by NO signaling.

Next, we tested how long the effect of ld-IL2 lasts after the cessation of treatment; and how NTG-induced facial hyper-sensitivity responds to the second round of ld-IL2 treatment. In male C57BL/6J mice, facial mechanical hyper-sensitivity was sustained by repeated NTG

injections for at least 4 weeks (Fig. 6D, NTG+saline), and was completely reversed by 7 daily ld-IL2 treatment (Fig. 6D, day 4–10). After cessation of IL2, it took two NTG injections (day 11–13) to lower the mechanical threshold to the level comparable to that of the NTG+saline group (Fig. 6D, day 15). We then started the second round of the daily ld-IL2 treatment (Fig. 6D, day 19–22). Notably, fewer ld-IL2 injections (4 versus 7 in the first session) were required to completely reverse NTG-induced mechanical hyper-sensitivity. We also compared the slope of reversal (change of threshold per day) between day 5–11 and day 19–23. The slope of ld-IL2-induced reversal was significantly steeper in the second session (10.3 ± 1.3, day 19–23) than the first (5.3 ± 0.9, day 5–11, $p < 0.01$, two-tailed t-test). Upon cessation of the second ld-IL2 treatment, it took 3 NTG injections (day 23–27) to reduce the withdrawal threshold to the level similar to that of the NTG+saline group (Fig. 6B, day 29). Taken together, we conclude that daily ld-IL2 can completely reverse the established persistent facial skin hyper-sensitivity resulting from repeated NTG administration, and the effect of IL2 occurs faster and lasts longer in mice with prior ld-IL2 treatment.

3.4. Treg cells mediate the therapeutic effect of ld-IL2.

To identify the cellular target of ld-IL2, we treated mice with an antibody against CD25, the IL2 receptor α chain that is highly expressed in Treg cells [11]. A single injection was sufficient to deplete 99% of Treg cells for 2 weeks without altering the facial mechanical thresholds at basal level or after NTG administration (Fig. 7A). In contrast, the effect of ld-IL2 was completely abolished in Treg-depleted mice (Fig. 7B). NTG-induced facial skin hyper-sensitivity persisted in CD25 antibody-treated mice throughout the course of ld-IL2 treatment (Fig. 7B, day 7–13), suggesting that endogenous Treg cells mediate the therapeutic effect of ld-IL2.

In addition to Treg cells, CD25 antibody may affect activated T cells in NTG-treated mice. We therefore tested whether adoptive transfer of Treg cells reverses NTG-induced skin hyper-sensitivity. We treated naïve C57BL/6J donor mice with ld-IL2 for 12 days, as previous work shows that Treg cells from IL2-treated mice exhibit stronger suppressive activity compared with those from saline-treated mice [56]. We then enriched CD25$^+$CD4$^+$ Treg cells from IL2-treated mice and adoptively transferred the cells to male C57BL/6J mice that had received 2 NTG injections and exhibited profound facial skin hyper-sensitivity to mechanical stimuli (Fig. 7C, day 4). The day before Treg transfer, the withdrawal threshold to von Frey filaments was about 14% of the baseline value (Fig. 7C, day 3). One day after the Treg transfer, the threshold was already increased to 70% of the baseline value (Fig. 7C, day 5). The effect of transferred Treg lasted for more than 15 days (Fig. 7C, day 5–21), so that the subsequent 7 NTG injections (day 5–17) completely failed to induce either acute (Fig. 7D) or persistent (Fig. 7C, day 7–19) mechanical hyper-sensitivity on facial skin. The frequency of CD25$^+$ Treg in the peripheral blood increased to $173 \pm 33\%$ of the baseline level on day 6 ($n = 4$ mice, $p < 0.05$, one-sample t-test), remained at $146 \pm 39\%$ on day 18 and returned to baseline level ($109 \pm 41\%$) by day 26. In control mice that received adoptive transfer of CD25$^-$CD4$^+$ T cells from IL2-treated mice, repeated NTG injections induced persistent facial skin mechanical hyper-sensitivity throughout the experiment (Fig. 7C). Similar to ld-IL2, Treg transfer did not alter baseline nociceptive responses to heat, cold or mechanical stimuli on facial skin or on hindpaw (Fig. 7E–I). This is consistent with the

working model that ld-IL2 reverses the effects of repeated NTG administration through targeting endogenous Treg cells.

To verify the purity of the transferred Treg cells, we conducted flow cytometry analysis on the enriched $CD25^+CD4^+$ Treg cells from DEREG mouse splenocytes. The preparations consisted of $92 \pm 4\%$ live cells, $97 \pm 1\%$ $CD4^+$ cells among live cells, $87 \pm 0.4\%$ $CD25^+$ cells among $CD4^+$ cells and $90 \pm 1\%$ $EGFP^+$ cells among $CD25^+CD4^+$ cells (n = 3 preparations, 2 mice per preparation), validating that the transferred cells were enriched in Treg. We also adoptively transferred Treg cells from IL2-treated DEREG mice to C57BL/6J recipient mice and used the EGFP signal to determine the tissue distribution of transferred Treg cells. $EGFP^+$ cells were present in the dura and TG 1 day after the adoptive transfer, and the level remained stable for at least 5 days (Fig. 8). In contrast, the cervical/medullary dorsal horn TCC of recipient mice contained few, if any, $EGFP^+$ cells (0–2 cells / mouse) during this time period, indicating that the transferred Tregs are located outside the brain while exerting their anti-migraine effects.

3.5. Ld-IL2 treatment inhibits mTBI-induced facial mechanical hyper-sensitivity and hyperalgesia priming.

PTH is a debilitating secondary headache disorder and is the most common medical consequence of mTBI [57]. Acute PTH occurs within 7 days of the injury. Persistent PTH lasts longer than 3 months to years after the trauma and often takes on a pattern of daily occurrence in the most severe cases [57]. We asked whether ld-IL2 can prevent and/or reverse PTH-related behaviors in a mouse model (Fig. 9A). In both male and female Swiss Webster mice, mTBI resulted in a significant reduction of the facial mechanical threshold (Fig. 9B, mTBI+saline groups, 3–28 days) which is mechanistically related to acute PTH [8,22,43]. There was no motor deficit as measured by rotarod, open field and adhesive removal tests between 6–12 days post-mTBI, when facial mechanical hyper-sensitivity reached the plateau (Fig. 10). After the mechanical thresholds returned to basal level 35 days post-mTBI, we treated mice with low dose NTG (0.1 mg/kg i.p.) daily for 4–6 days to mimic high frequency persistent PTH and measured the facial mechanical thresholds 1 day after the last NTG treatment [43]. Only mice that experienced mTBI developed facial mechanical hyper-sensitivity to repeated low-dose NTG (Fig. 9C, mTBI+saline groups), which is mechanistically related to mTBI-induced hyperalgesia priming during persistent PTH.

First, we treated female Swiss Webster mice with daily ld-IL2, starting 1 day post-mTBI for 9 days (Fig. 4A). This completely prevented the development of mTBI-induced acute facial mechanical hyper-sensitivity as well as the hyperalgesia priming revealed by repeated low-dose NTG (Fig. 9B–C, mTBI+IL2 groups). Next, we treated male Swiss Webster mice with daily ld-IL2 for 9 days, starting on post-mTBI day 7, when the facial mechanical threshold decreased to about 26% of the baseline value (Fig. 9D, The threshold returned to 87% of the baseline value after 3 days of ld-IL2 (Fig. 9D, day 10, mTBI+IL2 group), and mTBI-induced facial skin hyper-sensitivity was fully reversed by the end of ld-IL2 treatment (Fig. 9D, day 15). Daily ld-IL2 did not change the facial mechanical sensitivity of sham mice (Fig. 9D, sham+saline versus sham+IL2 groups). Importantly, 3 weeks after the cessation of ld-IL2, repeated low-dose NTG failed to establish persistent facial mechanical hyper-sensitivity in

mice that experienced mTBI (Fig. 9E, mTBI+saline versus mTBI+IL2 groups). Collectively, these results indicate that ld-IL2 treatment post-mTBI not only reverses injury-induced facial skin hyper-sensitivity but also prevents the development of hyperalgesia priming related to persistent PTH.

3.6. Ld-IL2 treatment reverses cutaneous mechanical hyper-sensitivity in a mouse model of MOH.

MOH is the most common secondary headache disorder, resulting from chronic and excessive use of medication to treat headache, for example, sumatriptan [20]. In both male and female C57BL/6J mice, daily administration of sumatriptan (0.6 mg/kg, i.p.) resulted in persistent facial and hindpaw mechanical hyper-sensitivity (Fig. 11A–D, SUMA+saline groups), consistent with previous reports [2,17,44]. Ld-IL2 treatment was initiated after mice received two sumatriptan injections, after the establishment of mechanical hyper-sensitivity (Fig. 11A–D, day 3). In both male and female mice, sumatriptan-induced cutaneous hyper-sensitivity was significantly attenuated after 4–6 ld-IL2 injections (Fig. 11, day 7–9), and was completely reversed after 8 days of IL2 treatment (Fig. 11, day 11). Moreover, with the continuous ld-IL2 treatment, neither male nor female mice developed cutaneous hyper-sensitivity in response to subsequent sumatriptan injections (Fig. 11, day 13). We conclude that ld-IL2 treatment not only reverses sumatriptan-induced behavioral sensitization, but also prevents the recurrence of sensitization by subsequent sumatriptan administrations.

4. Discussion

Recent years have seen significant advances in elucidating the mechanisms and in developing new therapy for chronic migraine and other headache disorders. Despite these exciting progresses, many patients remain either unresponsive to available treatments or intolerant to their side effects. Although numerous studies indicate that the activation of many pro-inflammatory immune cells contributes to the pathophysiology of migraine and PTH [9,37,41,48,51], the involvement of the immunosuppressive Treg cell in the chronification of headache disorders remains unknown. Many preclinical studies have identified ld-IL2 as a safe and effective treatment for multiple autoimmune and neurodegenerative diseases [16,30], but the potential of ld-IL2 as a therapy for headache disorders has not been explored. In this study, we employed multiple preclinical models and behavioral endpoints in male and female, inbred and outbred strains of mice to address these knowledge gaps. We report for the first time that repeated NTG administration significantly reduced the ratio of Treg cells among total T cells in TG, suggesting that chronic migraine is associated with a deficiency in Treg-mediated immune homeostasis in TG. Next, we tested the therapeutic use of ld-IL2 in mouse models of chronic migraine, PTH and MOH. Remarkably, in all these models, ld-IL2 treatment completely reversed the established facial skin hyper-sensitivity, which reflects the central sensitization under the chronic disease states. Continuous ld-IL2 treatment prevented the development of NTG- and sumatriptan-induced mechanical hyper-sensitivity related to chronic migraine and MOH, respectively. For behaviors related to mTBI-induced acute and persistent PTH, the therapeutic effect of ld-IL2 persisted after cessation of the treatment. The potential clinical significance of these

findings is that it provides the first proof-of-concept that ld-IL2 may constitute an innovative therapeutic strategy for the prevention and reversal of chronic migraine, PTH and MOH.

NTG administration is a well-established experimental model of migraine [18]. In migraineurs, NTG triggers migraine-like headache as well as cutaneous allodynia, and both are responsive to triptan treatment [1]. In rodents, both NTG-induced acute cutaneous allodynia and central sensitization can be blocked by sumatriptan and antagonists to calcitonin gene-related peptide (CGRP) receptor, suggesting that NTG-induced changes in rodents reflect the spontaneous migraine with cutaneous allodynia in some patients ([1,5,18] and references within). Repeated administration of NTG and other NO donors in rodents elicits persistent cutaneous allodynia that can be blocked by migraine prophylactics topiramate and propranolol [6,15,47], validating that these behavioral changes model symptoms of chronic migraine in humans. In the present study, we found that repeated NTG administration resulted in facial cold and mechanical hyper-sensitivity as well as hindpaw mechanical hyper-sensitivity, all of which were prevented by pre-treatment with ld-IL2. Starting ld-IL2 treatment after mice received repeated NTG administration completely reversed the established persistent facial mechanical hyper-sensitivity, regardless of mouse strain and sex. Continuous ld-IL2 treatment prevented subsequent NTG injections from re-establishing either acute or persistent cutaneous hyper-sensitivity. Collectively, these data predict that ld-IL2 treatment not only blocks trigger-induced migraine episodes, thereby preventing migraine chronification, but also induces the remission of chronic migraine in both males and females. Notably, a recent study reports that neither sumatriptan nor CGRP receptor antagonist olcegepant prevents the persistent cephalic mechanical hyper-sensitivity induced by repeated administration of NO donor isosorbide dinitrate [15], raising the possibility that ld-IL2 may be effective in reversing chronic migraine that is not responsive to drugs targeting CGRP signaling.

We did not attempt to determine the therapeutic window of ld-IL2 in mice, as the dose of IL2 required to activate/expand mouse and human Treg cells is very different, and numerous clinical trials have already established the appropriate dose of ld-IL2 in humans [30,49]. The dose of IL2 used in this study has been shown to preferentially expand and activate Treg cells in mice [30,56]. Indeed, we observed that daily ld-IL2 preferentially increased the frequency of Treg cells in the blood, LNs and spleen without altering the frequencies of $CD4^+$ and $CD3^+$ T cells. Moreover, ld-IL2 treatment increased the number of Treg cells in dura and TG by 4–9 folds, much higher than that seen in the blood, LNs or spleen. Results from Treg depletion and adoptive transfer experiments further validated Treg cell as the cellular target of ld-IL2. Depletion of endogenous Treg cells with anti-CD25 antibody did not alter the magnitude of NTG-induced mechanical hyper-sensitivity, likely due to the high dose of NTG used in our study. Whether Treg depletion alters the time course of NTG-induced behaviors and/or enhances the effects of lower dose of NTG merits further investigation.

In this study, we adoptively transferred Treg cells from IL2-treated mice. Further work will be needed to compare the efficacy of Treg cells from naïve mice and from IL2-treated mice. Notably, many exogenous Treg cells were present in the dura and TG 1 day after the adoptive transfer, whereas few Treg cells could be detected in the cervical/medullary dorsal

horn even 5 days after the transfer. Together, these results implicate dura and/or TG as sites of action for the therapeutic effect of ld-IL2 and Treg transfer, despite the fact that systemic NTG administration activates multiple pathways at both central and peripheral levels [18,24]. This is consistent with the recent studies indicating that both anti-CGRP antibodies and botulinum toxins act peripherally to reduce the frequency of migraine attacks [28,42].

In rodent models of nerve injury and EAE, mechanical allodynia was exacerbated by the depletion of Treg cells and was attenuated by the increase in Treg cell number [4,21,25,36,38]. The present study expanded the therapeutic value of ld-IL2 and Treg cells to chronic migraine and other headache disorders. Importantly, neither daily ld-IL2 treatment nor Treg transfer alters basal nociceptive responses, and the second round of ld-IL2 treatment reversed NTG-induced hyper-sensitivity faster and the effect lasted longer than the first round treatment. These data suggest that there is minimum risk of developing drug tolerance and/or MOH associated with ld-IL2 treatment. In fact, ld-IL2 completely reversed the facial as well as hindpaw hyper-sensitivity induced by daily injections of sumatriptan in both male and female mice. It is possible that ld-IL2 can reverse MOH resulting from repeated use of sumatriptan as well as other anti-migraine drugs, as a recent study shows that chronic exposure of rats to two acute headache medications with completely different mechanisms of action induced highly similar transcriptome changes in TG [10].

Treg cells are known to employ multiple mechanisms to exert suppressive activity and to maintain immune homeostasis, one of which is through enhancing the secretion of transforming growth factor β, interleukin-10 and/or interleukin-35 [52]. All of these cytokines have shown anti-nociceptive effects in chronic pain models [13,21,33,34]. Future study is warranted to determine whether ld-IL2 and Treg cells reverse nociceptive behaviors in various models of headache disorders through common or different mechanisms; whether it engages the secretion of individual cytokines and the regulation of the excitation of dural afferent neurons.

In rodent models of mTBI-induced PTH, the development of both acute and persistent PTH-related behaviors can be prevented by the repeated administration of anti-CGRP antibodies, starting immediately or 2 hours post-mTBI [8,45]. Discontinuing the anti-CGRP treatment after the resolution of mTBI-induced acute allodynia partially inhibits the development of hyperalgesia priming, and administration of anti-CGRP antibody after the resolution of acute allodynia fails to block the development of cutaneous allodynia in response to bright light stress [45]. In our model of mTBI-induced PTH, starting ld-IL2 treatment 1 day post-mTBI completely prevented the development of mTBI-induced acute facial mechanical hyper-sensitivity as well as the hyperalgesia priming revealed by repeated low-dose NTG. Notably, starting the 9-day ld-IL2 treatment after the acute hyper-sensitivity was fully established (7 days post-mTBI) could still completely prevent the development of hyperalgesia priming in addition to facilitating the resolution of acute mechanical hyper-sensitivity. In both cases, 9 days of ld-IL2 treatment was sufficient to protect both male and female mice from developing mTBI-induced hyperalgesia priming for at least 30 days. These results illustrate the potential of ld-IL2 as a novel therapy for mTBI-induced acute and persistent PTH, with a wide therapeutic time window and long-lasting beneficial effect after the cessation of the treatment. In addition to peripheral CGRP signaling, meningeal mast cell

is also involved in the development of mTBI-induced hyperalgesia priming [9]. Future in-depth studies are needed to elucidate whether the mechanisms of action of ld-IL2 involve interfering with the functions of CGRP and/or mast cells, and whether it involves peripheral and/or central sites. In addition, the effectiveness of ld-IL2 in other paradigms of mTBI-induced PTH merits further investigation.

Both reduction of Treg cell number and/or function in peripheral blood and decrease of serum IL2 level have been reported in migraine patients [3,46,55], supporting the clinical relevance of our study. There is abundant evidence from many clinical trials that both ld-IL2 treatment and Treg cell transfer are well tolerated in patients and show indications of efficacy against multiple autoimmune diseases [30,49,54]. The promising results for this preclinical study strongly support further clinical assessment of ld-IL2 treatment for multiple headache disorders including chronic migraine, PTH and MOH, and underline the high potential for rapid translation to clinical trials.

Supplementary Material

Refer to Web version on PubMed Central for supplementary material.

Acknowledgements

References

[1]. Akerman S, Karsan N, Bose P, Hoffmann JR, Holland PR, Romero-Reyes M, Goadsby PJ. Nitroglycerine triggers triptan-responsive cranial allodynia and trigeminal neuronal hypersensitivity. Brain : a journal of neurology 2019;142(1):103–119. [PubMed: 30596910]

[2]. Araldi D, Ferrari LF, Green P, Levine JD. Marked sexual dimorphism in 5-HT1 receptors mediating pronociceptive effects of sumatriptan. Neuroscience 2017;344:394–405. [PubMed: 28040566]

[3]. Arumugam M, Parthasarathy V. Reduction of CD4(+)CD25(+) regulatory T-cells in migraine: Is migraine an autoimmune disorder? Journal of neuroimmunology 2016;290:54–59. [PubMed: 26711570]

[4]. Austin PJ, Kim CF, Perera CJ, Moalem-Taylor G. Regulatory T cells attenuate neuropathic pain following peripheral nerve injury and experimental autoimmune neuritis. Pain 2012;153(9):1916–1931. [PubMed: 22789131]

[5]. Bates EA, Nikai T, Brennan KC, Fu YH, Charles AC, Basbaum AI, Ptacek LJ, Ahn AH. Sumatriptan alleviates nitroglycerin-induced mechanical and thermal allodynia in mice. Cephalalgia : an international journal of headache 2010;30(2):170–178. [PubMed: 19489890]

[6]. Ben Aissa M, Tipton AF, Bertels Z, Gandhi R, Moye LS, Novack M, Bennett BM, Wang Y, Litosh V, Lee SH, Gaisina IN, Thatcher GR, Pradhan AA. Soluble guanylyl cyclase is a critical regulator of migraine-associated pain. Cephalalgia : an international journal of headache 2018;38(8):1471–1484. [PubMed: 29022756]

[7]. Bouet V, Boulouard M, Toutain J, Divoux D, Bernaudin M, Schumann-Bard P, Freret T. The adhesive removal test: a sensitive method to assess sensorimotor deficits in mice. Nature protocols 2009;4(10):1560–1564. [PubMed: 19798088]

[8]. Bree D, Levy D. Development of CGRP-dependent pain and headache related behaviours in a rat model of concussion: Implications for mechanisms of post-traumatic headache. Cephalalgia : an international journal of headache 2018;38(2):246–258. [PubMed: 27899434]

[9]. Bree D, Levy D. Intact mast cell content during mild head injury is required for development of latent pain sensitization: implications for mechanisms underlying post-traumatic headache. Pain 2019;160(5):1050–1058. [PubMed: 30624345]

[10]. Buonvicino D, Urru M, Muzzi M, Ranieri G, Luceri C, Oteri C, Lapucci A, Chiarugi A. Trigeminal ganglion transcriptome analysis in 2 rat models of medication-overuse headache reveals coherent and widespread induction of pronociceptive gene expression patterns. Pain 2018;159(10):1980–1988. [PubMed: 29794878]

[11]. Cao X, Cai SF, Fehniger TA, Song J, Collins LI, Piwnica-Worms DR, Ley TJ. Granzyme B and perforin are important for regulatory T cell-mediated suppression of tumor clearance. Immunity 2007;27(4):635–646. [PubMed: 17919943]

[12]. Chaplan SR, Bach FW, Pogrel JW, Chung JM, Yaksh TL. Quantitative assessment of tactile allodynia in the rat paw. Journal of neuroscience methods 1994;53(1):55–63. [PubMed: 7990513]

[13]. Chen G, Park CK, Xie RG, Ji RR. Intrathecal bone marrow stromal cells inhibit neuropathic pain via TGF-beta secretion. The Journal of clinical investigation 2015;125(8):3226–3240. [PubMed: 26168219]

[14]. Constandil L, Goich M, Hernandez A, Bourgeais L, Cazorla M, Hamon M, Villanueva L, Pelissier T. Cyclotraxin-B, a new TrkB antagonist, and glial blockade by propentofylline, equally prevent and reverse cold allodynia induced by BDNF or partial infraorbital nerve constriction in mice. The journal of pain : official journal of the American Pain Society 2012;13(6):579–589. [PubMed: 22560237]

[15]. Dallel R, Descheemaeker A, Luccarini P. Recurrent administration of the nitric oxide donor, isosorbide dinitrate, induces a persistent cephalic cutaneous hypersensitivity: A model for migraine progression. Cephalalgia : an international journal of headache 2018;38(4):776–785. [PubMed: 28565942]

[16]. Dansokho C, Ait Ahmed D, Aid S, Toly-Ndour C, Chaigneau T, Calle V, Cagnard N, Holzenberger M, Piaggio E, Aucouturier P, Dorothee G. Regulatory T cells delay disease progression in Alzheimer-like pathology. Brain : a journal of neurology 2016;139(Pt 4):1237–1251. [PubMed: 26912648]

[17]. De Felice M, Ossipov MH, Wang R, Lai J, Chichorro J, Meng I, Dodick DW, Vanderah TW, Dussor G, Porreca F. Triptan-induced latent sensitization: a possible basis for medication overuse headache. Annals of neurology 2010;67(3):325–337. [PubMed: 20373344]

[18]. Demartini C, Greco R, Zanaboni AM, Sances G, De Icco R, Borsook D, Tassorelli C. Nitroglycerin as a comparative experimental model of migraine pain: From animal to human and back. Progress in neurobiology 2019;177:15–32. [PubMed: 30771365]

[19]. Di W, Shi X, Lv H, Liu J, Zhang H, Li Z, Fang Y. Activation of the nuclear factor E2-related factor 2/anitioxidant response element alleviates the nitroglycerin-induced hyperalgesia in rats. The journal of headache and pain 2016;17(1):99. [PubMed: 27778243]

[20]. Diener HC, Holle D, Solbach K, Gaul C. Medication-overuse headache: risk factors, pathophysiology and management. Nature reviews Neurology 2016;12(10):575–583. [PubMed: 27615418]

[21]. Duffy SS, Keating BA, Perera CJ, Lees JG, Tonkin RS, Makker PGS, Carrive P, Butovsky O, Moalem-Taylor G. Regulatory T Cells and Their Derived Cytokine, Interleukin-35, Reduce Pain in Experimental Autoimmune Encephalomyelitis. The Journal of neuroscience : the official journal of the Society for Neuroscience 2019;39(12):2326–2346.

[22]. Elliott MB, Oshinsky ML, Amenta PS, Awe OO, Jallo JI. Nociceptive neuropeptide increases and periorbital allodynia in a model of traumatic brain injury. Headache 2012;52(6):966–984. [PubMed: 22568499]

[23]. Farkas S, Bolcskei K, Markovics A, Varga A, Kis-Varga A, Kormos V, Gaszner B, Horvath C, Tuka B, Tajti J, Helyes Z. Utility of different outcome measures for the nitroglycerin model of migraine in mice. Journal of pharmacological and toxicological methods 2016;77:33–44. [PubMed: 26456070]

[24]. Ferrari LF, Levine JD, Green PG. Mechanisms mediating nitroglycerin-induced delayed-onset hyperalgesia in the rat. Neuroscience 2016;317:121–129. [PubMed: 26779834]

[25]. Fischer R, Sendetski M, Del Rivero T, Martinez GF, Bracchi-Ricard V, Swanson KA, Pruzinsky EK, Delguercio N, Rosalino MJ, Padutsch T, Kontermann RE, Pfizenmaier K, Bethea JR. TNFR2 promotes Treg-mediated recovery from neuropathic pain across sexes. Proceedings of the National Academy of Sciences of the United States of America 2019;116(34):17045–17050. [PubMed: 31391309]

[26]. Hartemann A, Bensimon G, Payan CA, Jacqueminet S, Bourron O, Nicolas N, Fonfrede M, Rosenzwajg M, Bernard C, Klatzmann D. Low-dose interleukin 2 in patients with type 1 diabetes: a phase 1/2 randomised, double-blind, placebo-controlled trial. The lancet Diabetes & endocrinology 2013;1(4):295–305. [PubMed: 24622415]

[27]. Huang D, Ren L, Qiu CS, Liu P, Peterson J, Yanagawa Y, Cao YQ. Characterization of a mouse model of headache. Pain 2016;157(8):1744–1760. [PubMed: 27058678]

[28]. Johnson KW, Morin SM, Wroblewski VJ, Johnson MP. Peripheral and central nervous system distribution of the CGRP neutralizing antibody [(125)I] galcanezumab in male rats. Cephalalgia : an international journal of headache 2019;39(10):1241–1248. [PubMed: 31003588]

[29]. Kim SJ, Yeo JH, Yoon SY, Kwon SG, Lee JH, Beitz AJ, Roh DH. Differential Development of Facial and Hind Paw Allodynia in a Nitroglycerin-Induced Mouse Model of Chronic Migraine: Role of Capsaicin Sensitive Primary Afferents. Biological & pharmaceutical bulletin 2018;41(2):172–181. [PubMed: 29187670]

[30]. Klatzmann D, Abbas AK. The promise of low-dose interleukin-2 therapy for autoimmune and inflammatory diseases. Nature reviews Immunology 2015;15(5):283–294.

[31]. Kopruszinski CM, Xie JY, Eyde NM, Remeniuk B, Walter S, Stratton J, Bigal M, Chichorro JG, Dodick D, Porreca F. Prevention of stress- or nitric oxide donor-induced medication overuse headache by a calcitonin gene-related peptide antibody in rodents. Cephalalgia : an international journal of headache 2017;37(6):560–570. [PubMed: 27206958]

[32]. Koreth J, Matsuoka K, Kim HT, McDonough SM, Bindra B, Alyea EP 3rd, Armand P, Cutler C, Ho VT, Treister NS, Bienfang DC, Prasad S, Tzachanis D, Joyce RM, Avigan DE, Antin JH, Ritz J, Soiffer RJ. Interleukin-2 and regulatory T cells in graft-versus-host disease. The New England journal of medicine 2011;365(22):2055–2066. [PubMed: 22129252]

[33]. Krukowski K, Eijkelkamp N, Laumet G, Hack CE, Li Y, Dougherty PM, Heijnen CJ, Kavelaars A. CD8+ T Cells and Endogenous IL-10 Are Required for Resolution of Chemotherapy-Induced Neuropathic Pain. The Journal of neuroscience : the official journal of the Society for Neuroscience 2016;36(43):11074–11083. [PubMed: 27798187]

[34]. Kwilasz AJ, Grace PM, Serbedzija P, Maier SF, Watkins LR. The therapeutic potential of interleukin-10 in neuroimmune diseases. Neuropharmacology 2015;96(Pt A):55–69. [PubMed: 25446571]

[35]. Lahl K, Loddenkemper C, Drouin C, Freyer J, Arnason J, Eberl G, Hamann A, Wagner H, Huehn J, Sparwasser T. Selective depletion of Foxp3+ regulatory T cells induces a scurfy-like disease. The Journal of experimental medicine 2007;204(1):57–63. [PubMed: 17200412]

[36]. Lees JG, Duffy SS, Perera CJ, Moalem-Taylor G. Depletion of Foxp3+ regulatory T cells increases severity of mechanical allodynia and significantly alters systemic cytokine levels following peripheral nerve injury. Cytokine 2015;71(2):207–214. [PubMed: 25461400]

[37]. Levy D, Burstein R, Kainz V, Jakubowski M, Strassman AM. Mast cell degranulation activates a pain pathway underlying migraine headache. Pain 2007;130(1–2):166–176. [PubMed: 17459586]

[38]. Liu XJ, Zhang Y, Liu T, Xu ZZ, Park CK, Berta T, Jiang D, Ji RR. Nociceptive neurons regulate innate and adaptive immunity and neuropathic pain through MyD88 adapter. Cell research 2014;24(11):1374–1377. [PubMed: 25112711]

[39]. Marone IM, De Logu F, Nassini R, De Carvalho Goncalves M, Benemei S, Ferreira J, Jain P, Li Puma S, Bunnett NW, Geppetti P, Materazzi S. TRPA1/NOX in the soma of trigeminal ganglion neurons mediates migraine-related pain of glyceryl trinitrate in mice. Brain : a journal of neurology 2018;141(8):2312–2328. [PubMed: 29985973]

[40]. May A, Schulte LH. Chronic migraine: risk factors, mechanisms and treatment. Nature reviews Neurology 2016;12(8):455–464. [PubMed: 27389092]

[41]. McIlvried LA, Cruz JA, Borghesi LA, Gold MS. Sex-, stress-, and sympathetic post-ganglionic-dependent changes in identity and proportions of immune cells in the dura. Cephalalgia : an international journal of headache 2017;37(1):36–48. [PubMed: 26970607]

[42]. Melo-Carrillo A, Strassman AM, Schain AJ, Noseda R, Ashina S, Adams A, Brin MF, Burstein R. Exploring the effects of extracranial injections of botulinum toxin type A on prolonged intracranial meningeal nociceptors responses to cortical spreading depression in female rats. Cephalalgia : an international journal of headache 2019;39(11):1358–1365. [PubMed: 31475573]

[43]. Moye LS, Novack ML, Tipton AF, Krishnan H, Pandey SC, Pradhan AA. The development of a mouse model of mTBI-induced post-traumatic migraine, and identification of the delta opioid receptor as a novel therapeutic target. Cephalalgia : an international journal of headache 2019;39(1):77–90. [PubMed: 29771142]

[44]. Moye LS, Tipton AF, Dripps I, Sheets Z, Crombie A, Violin JD, Pradhan AA. Delta opioid receptor agonists are effective for multiple types of headache disorders. Neuropharmacology 2019;148:77–86. [PubMed: 30553828]

[45]. Navratilova E, Rau J, Oyarzo J, Tien J, Mackenzie K, Stratton J, Remeniuk B, Schwedt T, Anderson T, Dodick D, Porreca F. CGRP-dependent and independent mechanisms of acute and persistent post-traumatic headache following mild traumatic brain injury in mice. Cephalalgia : an international journal of headache 2019:333102419877662.

[46]. Nurkhametova D, Kudryavtsev I, Khayrutdinova O, Serebryakova M, Altunbaev R, Malm T, Giniatullin R. Purinergic Profiling of Regulatory T-cells in Patients With Episodic Migraine. Frontiers in cellular neuroscience 2018;12:326. [PubMed: 30319363]

[47]. Pradhan AA, Smith ML, McGuire B, Tarash I, Evans CJ, Charles A. Characterization of a novel model of chronic migraine. Pain 2014;155(2):269–274. [PubMed: 24121068]

[48]. Reuter U, Bolay H, Jansen-Olesen I, Chiarugi A, Sanchez del Rio M, Letourneau R, Theoharides TC, Waeber C, Moskowitz MA. Delayed inflammation in rat meninges: implications for migraine pathophysiology. Brain : a journal of neurology 2001;124(Pt 12):2490–2502. [PubMed: 11701602]

[49]. Rosenzwajg M, Lorenzon R, Cacoub P, Pham HP, Pitoiset F, El Soufi K, C RI, Bernard C, Aractingi S, Banneville B, Beaugerie L, Berenbaum F, Champey J, Chazouilleres O, Corpechot C, Fautrel B, Mekinian A, Regnier E, Saadoun D, Salem JE, Sellam J, Seksik P, Daguenel-Nguyen A, Doppler V, Mariau J, Vicaut E, Klatzmann D. Immunological and clinical effects of low-dose interleukin-2 across 11 autoimmune diseases in a single, open clinical trial. Annals of the rheumatic diseases 2019;78(2):209–217. [PubMed: 30472651]

[50]. Saadoun D, Rosenzwajg M, Joly F, Six A, Carrat F, Thibault V, Sene D, Cacoub P, Klatzmann D. Regulatory T-cell responses to low-dose interleukin-2 in HCV-induced vasculitis. The New England journal of medicine 2011;365(22):2067–2077. [PubMed: 22129253]

[51]. Schain AJ, Melo-Carrillo A, Borsook D, Grutzendler J, Strassman AM, Burstein R. Activation of pial and dural macrophages and dendritic cells by cortical spreading depression. Annals of neurology 2018;83(3):508–521. [PubMed: 29394508]

[52]. Schmidt A, Oberle N, Krammer PH. Molecular mechanisms of treg-mediated T cell suppression. Frontiers in immunology 2012;3:51. [PubMed: 22566933]

[53]. Setiady YY, Coccia JA, Park PU. In vivo depletion of CD4+FOXP3+ Treg cells by the PC61 anti-CD25 monoclonal antibody is mediated by FcgammaRIII+ phagocytes. European journal of immunology 2010;40(3):780–786. [PubMed: 20039297]

[54]. Sharabi A, Tsokos MG, Ding Y, Malek TR, Klatzmann D, Tsokos GC. Regulatory T cells in the treatment of disease. Nature reviews Drug discovery 2018.

[55]. Shimomura T, Araga S, Esumi E, Takahashi K. Decreased serum interleukin-2 level in patients with chronic headache. Headache 1991;31(5):310–313. [PubMed: 1860789]

[56]. Tahvildari M, Omoto M, Chen Y, Emami-Naeini P, Inomata T, Dohlman TH, Kaye AE, Chauhan SK, Dana R. In Vivo Expansion of Regulatory T Cells by Low-Dose Interleukin-2 Treatment Increases Allograft Survival in Corneal Transplantation. Transplantation 2016;100(3):525–532. [PubMed: 26881788]

[57]. Yilmaz T, Roks G, de Koning M, Scheenen M, van der Horn H, Plas G, Hageman G, Schoonman G, Spikman J, van der Naalt J. Risk factors and outcomes associated with post-traumatic

headache after mild traumatic brain injury. Emergency medicine journal : EMJ 2017;34(12):800–805. [PubMed: 28689194]

[58]. Zohar O, Schreiber S, Getslev V, Schwartz JP, Mullins PG, Pick CG. Closed-head minimal traumatic brain injury produces long-term cognitive deficits in mice. Neuroscience 2003;118(4):949–955. [PubMed: 12732240]
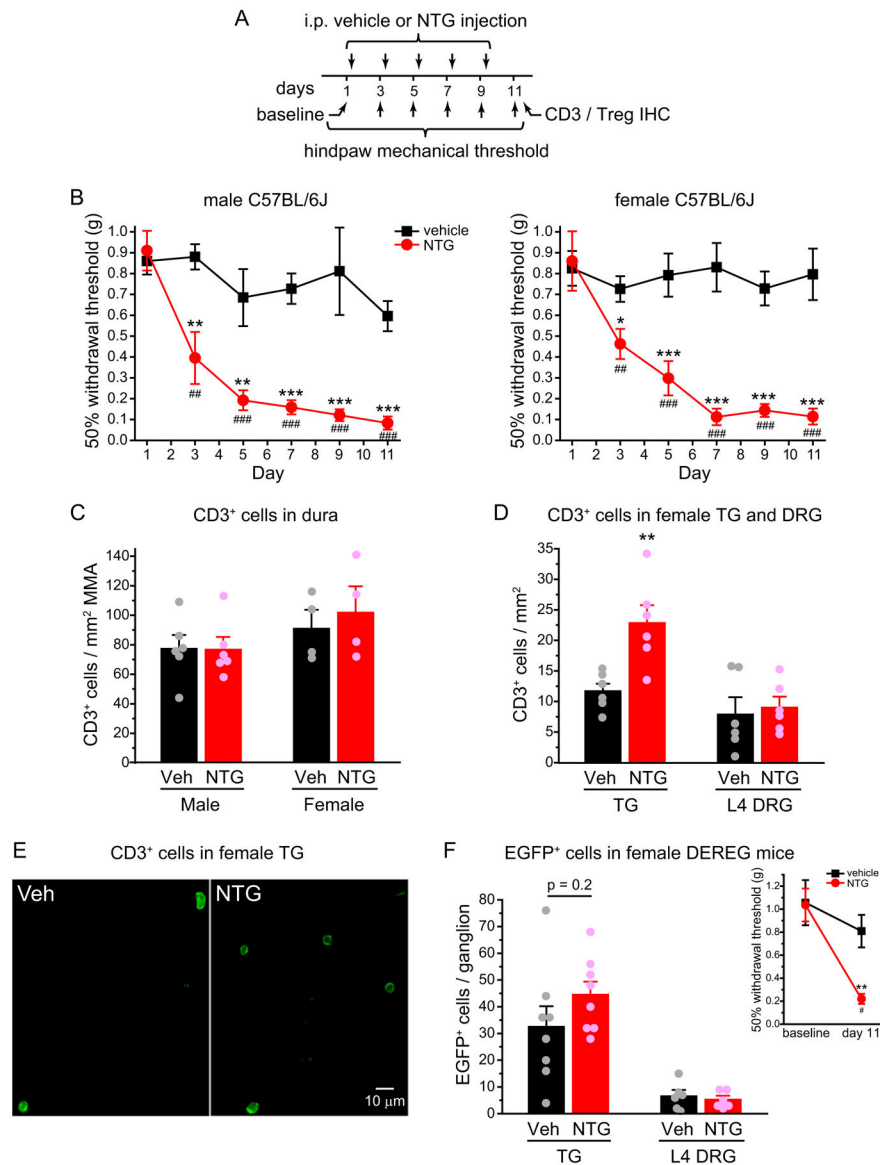
Figure 1. Repeated NTG treatment increases the number of CD3$^+$ cells but not Treg cells in mouse TG.

(A) Time line of experiments. Note that NTG was always injected after the completion of behavioral tests on the same day.

(B) Repetitive NTG treatment (10 mg/kg, i.p.) induces progressive and sustained hindpaw mechanical hyper-sensitivity in both male (left, n = 6/group) and female C57BL/6J mice (right, n = 8/group). Kruskal-Wallis ANOVA on ranks with post hoc Student-Newman-Keuls test: *p < 0.05, **p < 0.01, ***p < 0.001, between the corresponding vehicle and NTG groups. Friedman test: p < 0.05 and p < 0.001 within the male and female NTG groups, respectively, $^{\#\#}$p < 0.01, $^{\#\#\#}$p < 0.001, compared with the baseline threshold (day 1).

(C) The density of CD3$^+$ cells in the dura surrounding the MMA in male (n = 6/group) and female C57BL/6J mice (n = 4/group) that received repetitive vehicle and NTG injections, respectively.

(D) The density of CD3$^+$ cells in the TG (n = 6/group) and L4 DRG (n = 6/group) of female C57BL/6J mice receiving repetitive vehicle and NTG injections, respectively. **p < 0.01, two-tailed t-test between the corresponding vehicle and NTG groups.

(E) Representative images of CD3$^+$ cells in TG sections from female C57BL/6J mice that received repetitive vehicle or NTG injections (same mice as in **D**).

(F) The number of EGFP$^+$ Treg cells per TG (n = 8/group) and per L4 DRG (n = 6/group) from female DEREG mice that received repetitive vehicle and NTG injections, respectively. Inset: The 50% withdrawal thresholds to von Frey filaments on the hindpaw of female DEREG mice (n = 4/group) before and two days after the last NTG or vehicle injections as shown in **A**. Kruskal-Wallis ANOVA on ranks with post hoc Student-Newman-Keuls test: **p < 0.01, between the corresponding vehicle and NTG groups; #p < 0.05, between the NTG-treated groups.
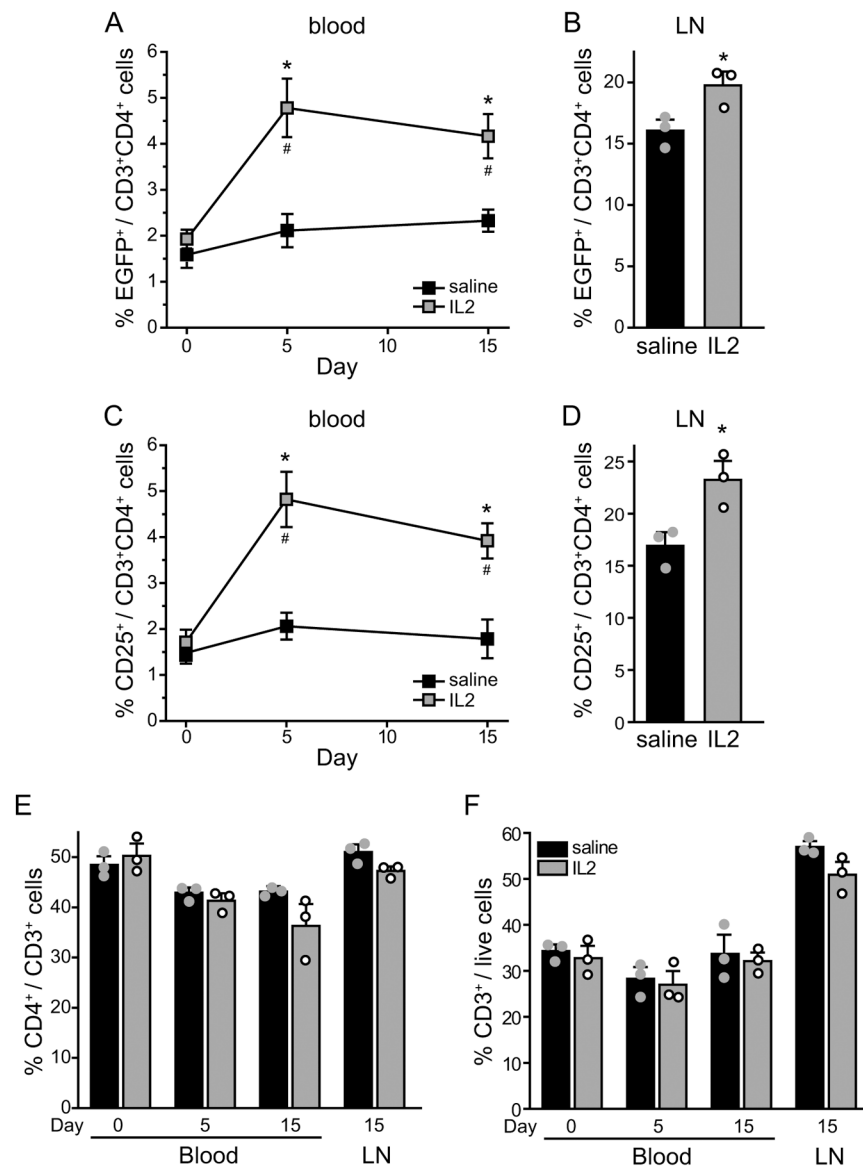
Figure 2. The frequencies of CD3+, CD4+ and Treg cells in the peripheral blood and cervical LNs of DEREG mice treated with daily saline or ld-IL2.

(**A**) The percentage of EGFP+ Treg cells among CD4+CD3+ T cells in the peripheral blood of male DEREG mice that received 15 daily injections of saline and ld-IL2, respectively (n = 3/group). The injections started on day 0, after blood collection for baseline measurement. Two-way RM ANOVA with post hoc Bonferroni test: *p < 0.05, between the corresponding saline and IL2 groups; #p < 0.05, compared with the baseline value (day 0) in the IL2 group.
(**B**) The frequency of EGFP+ Treg cells among CD4+CD3+ T cells in the cervical LNs after 15 daily saline or ld-IL2 injections (same mice as in **A**). *p < 0.05, two-tailed t-test.
(**C**) The percentage of CD25+ Treg cells among CD4+CD3+ T cells in the peripheral blood of saline- and IL2-treated DEREG mice (same as in **A**). Two-way RM ANOVA with post hoc Bonferroni test: *p < 0.05, between the corresponding saline and IL2 groups; #p < 0.05, compared with the baseline value (day 0) in the IL2 group.

(D) The frequency of CD25$^+$ Treg among CD4$^+$CD3$^+$ cells in the cervical LNs after 15 daily saline or ld-IL2 injections (same mice as in **A**). *p < 0.05, two-tailed t-test.

(E-F) The abundance of CD4$^+$ cells among CD3$^+$ cells (**E**) and CD3$^+$ cells among live lymphocytes (**F**) in saline- and IL2-treated mice (same as in **A**).
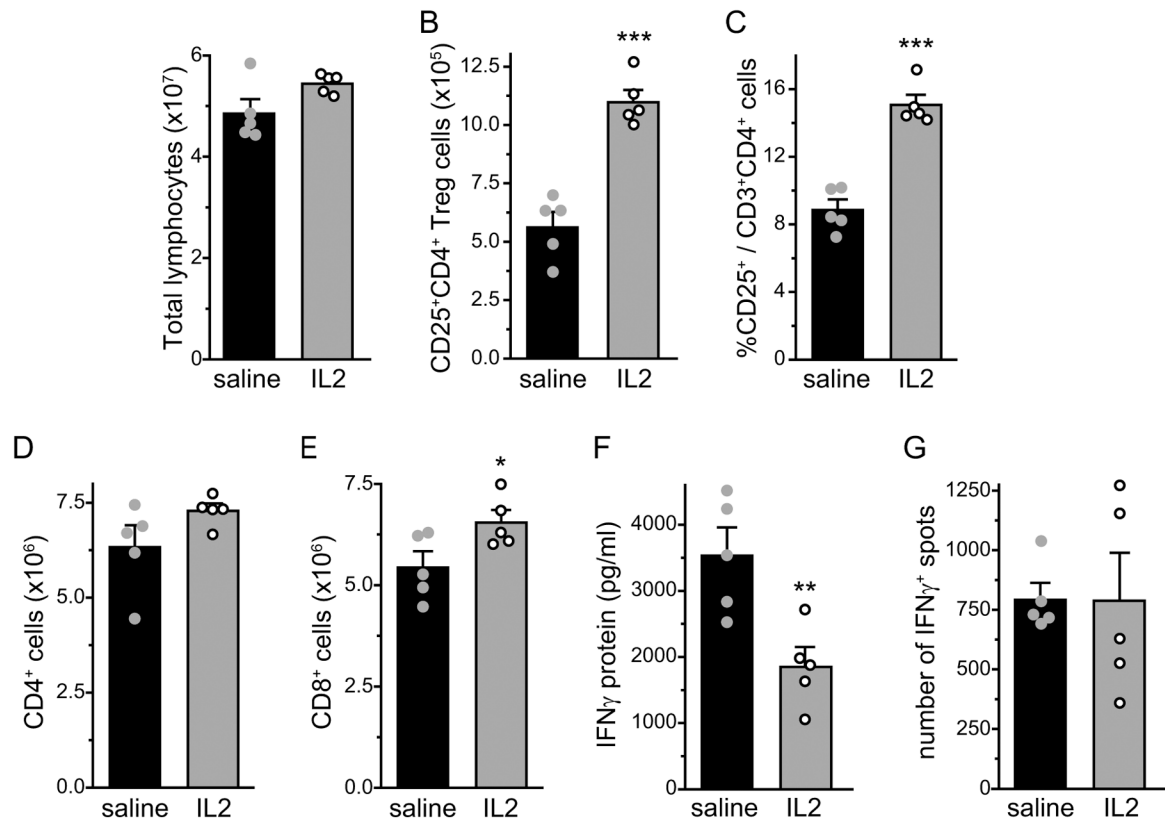
Figure 3. Analysis of splenocytes from mice treated with daily saline or ld-IL2.

(A-B) The number of lymphocytes (**A**) and CD25$^+$CD4$^+$ Treg cells (**B**) in total splenocytes of male C57BL6/J mice that received 15 daily injections of saline and ld-IL2, respectively (n = 5 mice/group). ***p < 0.001, two-tailed t-test.

(**C**) The frequency (**C**) of CD25$^+$ Treg cells among CD3$^+$CD4$^+$ splenocytes from saline- and IL2-treated mice (same as in **A**). ***p < 0.001, two-tailed t-test.

(**D-E**) The number of CD3$^+$CD4$^+$ cells (**D**) and CD3$^+$CD8$^+$ cells (**E**) in splenocytes from saline- and IL2-treated mice (same as in **A**). *p < 0.05, two-tailed t-test.

(F) The secretion of IFNγ in response to CD3/CD28 stimulation in ELISA assay (n = 5/ group, same as in **A**). **p < 0.01, two-tailed t-test.

(G) The number of INFγ-secreting (IFNγ^+) cells in splenocytes from saline- and IL2-treated mice (same as in **A**).
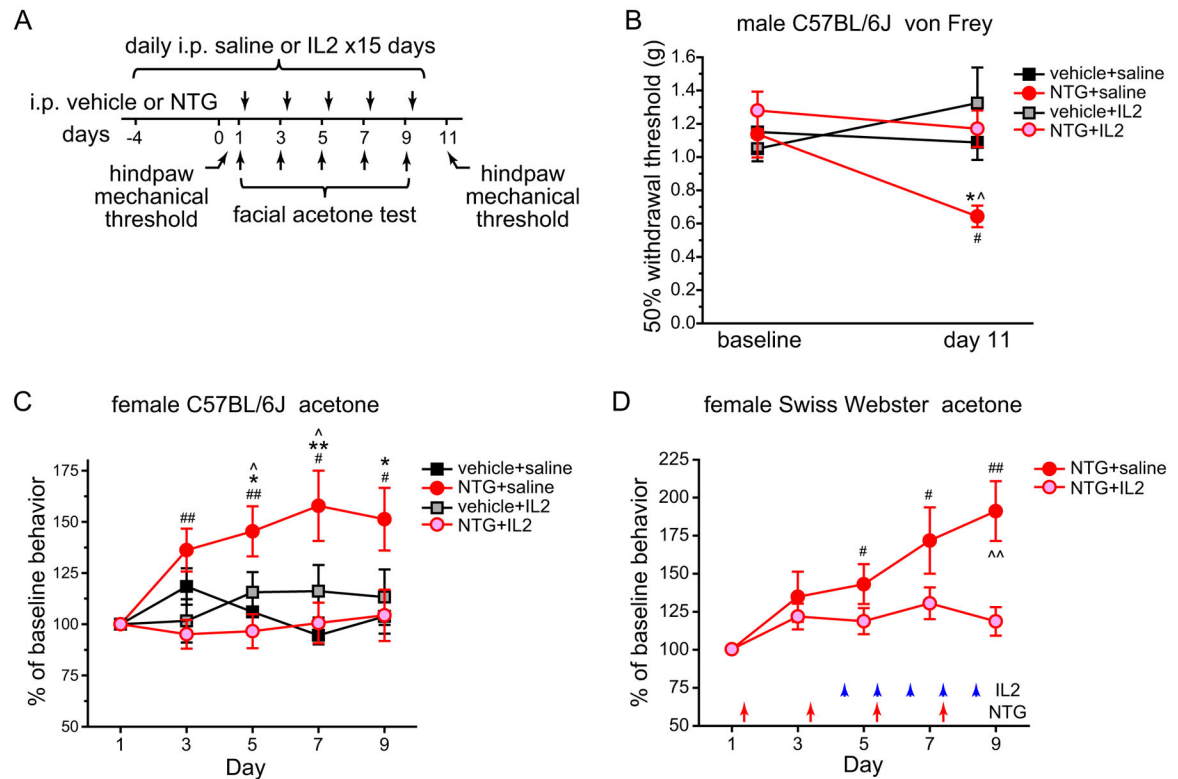
Figure 4. Pretreatment with ld-IL2 prevents the development of NTG-induced skin hyper-sensitivity.

(**A**) Time line of experiments in **B** and **C**. Note that IL2 and/or NTG were always injected after the completion of behavioral tests on the same day.

(**B**) Hindpaw mechanical thresholds of male C57BL/6J mice at baseline and two days after the last NTG or vehicle injections as shown in **A** (n = 6, 7, 6 and 5 mice in vehicle, NTG, vehicle+IL2 and NTG+IL2 groups, respectively). Kruskal-Wallis ANOVA on ranks with Student-Newman-Keuls post hoc test. *p < 0.05, between the vehicle+saline and NTG +saline groups on day 11; ^p < 0.05, between the NTG+saline and NTG+IL2 groups on day 11; #p < 0.05, between the baseline and day 11 NTG+saline groups.

(**C**) The effects of repetitive NTG and/or ld-IL2 on the duration of acetone-induced cheek wiping in female C57BL/6J mice (n = 14, 20, 9 and 12 in vehicle+saline, NTG+saline, vehicle+IL2 and NTG+IL2 groups, respectively). The duration of wiping was normalized to the baseline values (day 1) in individual mice. Two-way RM ANOVA: p < 0.01; post hoc t-test with Bonferroni correction: *p < 0.05, **p < 0.01, between the corresponding vehicle and NTG groups; ^p < 0.05, between the corresponding NTG+saline and NTG+IL2 groups; one-way RM ANOVA: p < 0.05 within the NTG+saline group, post hoc one-sample t-test with Bonferroni correction: #p < 0.05, ##p < 0.01, compared with the baseline.

(**D**) The effects of repetitive NTG and/or ld-IL2 on the duration of acetone-induced cheek wiping in female Swiss Webster mice (n = 8 and 11 in NTG+saline and NTG+IL2 groups, respectively). The duration of wiping was normalized to the baseline values (day 1) in individual mice. Arrows and arrowheads indicate the injections of NTG and IL2, respectively. Two-way RM ANOVA: p < 0.05; post hoc t-test with Bonferroni correction: ^^p < 0.01, between the corresponding NTG+saline and NTG+IL2 groups; one-way RM

ANOVA: p < 0.001 within the NTG+saline group, post hoc one-sample t-test with Bonferroni correction: [#]p < 0.05, [##]p < 0.01, compared with the baseline.
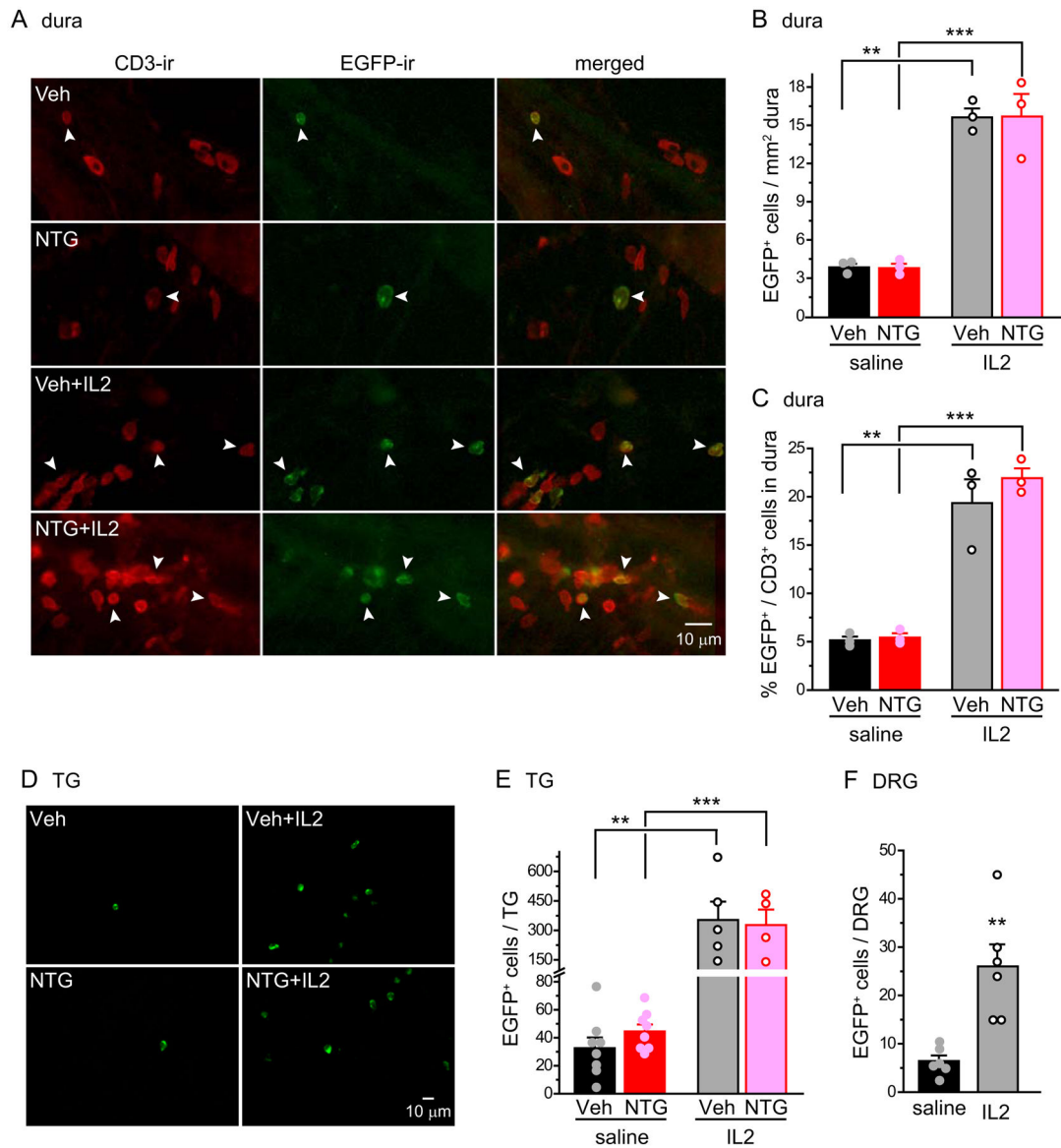
Figure 5. Ld-IL2 treatment increases the number of Treg cells in dura and TG.

(A) Representative images of EGFP$^+$ Treg cells and CD3$^+$ cells in the dura of DEREG mice that received repeated NTG and/or ld-IL2 administrations. Arrowheads indicate double-labeled CD3$^+$EGFP$^+$ Treg cells.

(B-C) Daily ld-IL2 treatment (x 15 days) significantly increases the number of EGFP$^+$ Treg cells **(B)** and the frequency of EGFP$^+$ Treg among CD3$^+$ T cells **(C)** in the dura surrounding the MMA of male DEREG mice (n = 3/group). **p < 0.01, **p < 0.001, two-way ANOVA with post hoc Bonferroni test.

(D) Representative images of EGFP$^+$ Treg cells in the TG of DEREG mice that received repeated NTG and/or ld-IL2 administrations.

(E) Daily ld-IL2 treatment (x 15 days) significantly increases the number of EGFP$^+$ Treg cells in the TG of female DEREG mice (n = 5 and 4 mice in vehicle+IL2 and NTG+IL2

groups; vehicle+saline and NTG+saline groups: same mice as in Fig. 1F). **p < 0.01, ***p < 0.001, two-way ANOVA with post hoc Bonferroni test.

(F) Daily ld-IL2 treatment (x 15 days) significantly increases the number of EGFP⁺ Treg cells in the DRG of male DEREG mice (n = 6/group). **p < 0.01, two-tailed t-test.

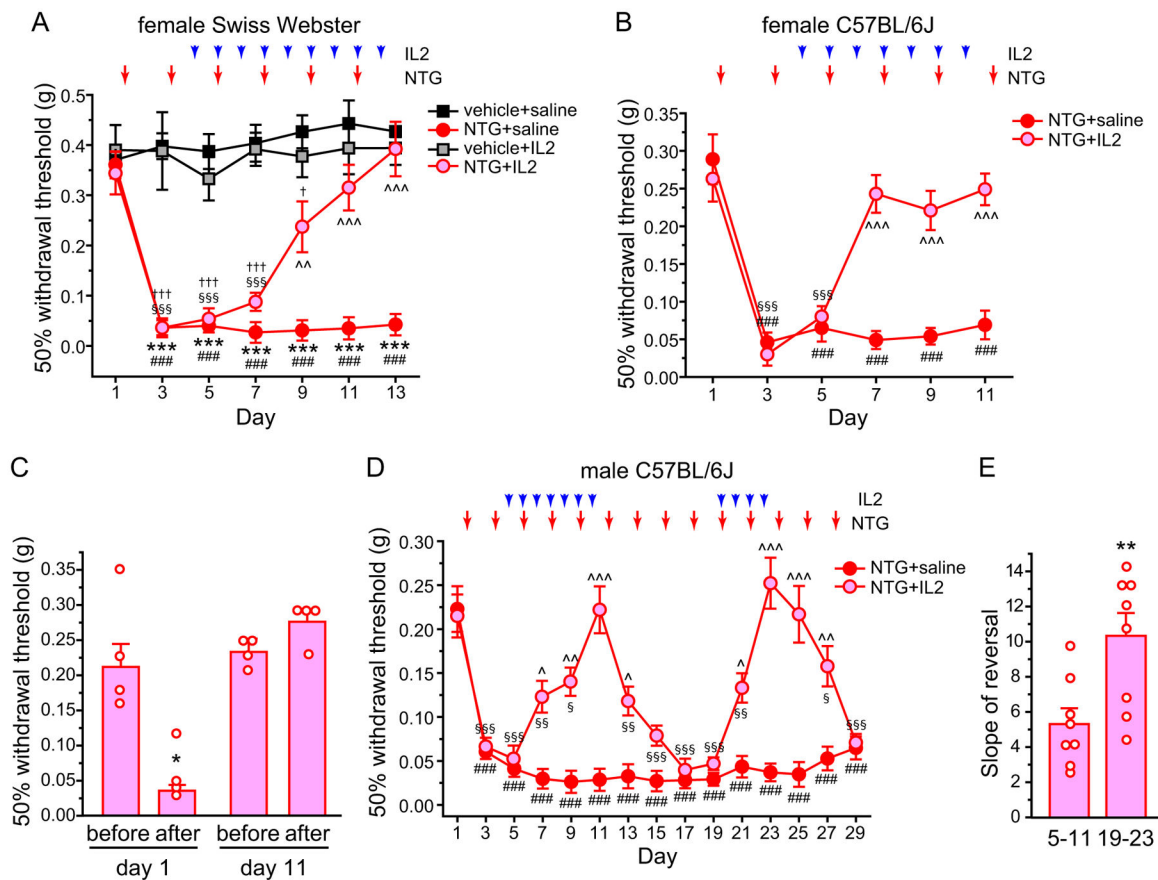**Figure 6. NTG-induced persistent skin hyper-sensitivity is reversed by ld-IL2 treatment.**
(A) The effects of repetitive NTG and/or ld-IL2 on the 50% withdrawal thresholds to von Frey filaments at the periorbital region of female Swiss Webster mice (n = 6, 6, 5 and 9 in vehicle+saline, NTG+saline, vehicle+IL2 and NTG+IL2 groups, respectively). Arrows and arrowheads indicate the injections of NTG and IL2, respectively. Note that IL2 and NTG were always injected after the completion of behavioral tests on the same day. Kruskal-Wallis ANOVA on ranks: $p < 0.05$; post hoc Student-Newman-Keuls test: ***$p < 0.001$, between the corresponding vehicle+saline and NTG+saline groups; ^^$p < 0.01$, ^^^$p < 0.001$, between the corresponding NTG+saline and NTG+IL2 groups; †$p < 0.05$, †††$p < 0.001$, between the corresponding NTG+IL2 and vehicle+IL2 groups; Friedman test: $p < 0.05$ within the NTG+saline group, ###$p < 0.001$, compared with the baseline threshold (day 1); $p < 0.001$ within the NTG+IL2 group, §§§$p < 0.001$, compared with the baseline threshold (day 1).
(B) The effects of repeated NTG and/or ld-IL2 on the facial mechanical thresholds of female C57BL/6J mice (n = 5 and 6 in NTG+saline and NTG+IL2 groups, respectively). Kruskal-Wallis ANOVA on ranks: $p < 0.05$; post hoc Student-Newman-Keuls test: ^^^$p < 0.001$, between the corresponding NTG+saline and NTG+IL2 groups; Friedman test: $p < 0.05$ within the NTG+saline group, ###$p < 0.001$, compared with the baseline threshold (day 1); $p < 0.001$ within the NTG+IL2 group, §§§$p < 0.001$, compared with the baseline threshold (day 1).

(C) In 4 mice (out of the 6 mice in **B** NTG+IL2 group), facial mechanical thresholds before and 3 hours after NTG injections were measured on day 1 (before ld-IL2) and day 11 (after 7 ld-IL2 injections). *p < 0.05, Mann–Whitney U test comparing naïve mice before and after NTG treatment.

(D) The effects of repeated NTG and/or ld-IL2 on the facial mechanical thresholds of male C57BL/6J mice (n = 6 and 9 in NTG+saline and NTG+IL2 groups, respectively). NTG was injected every two days throughout the experiment. Mice in the NTG+IL2 group received two sessions of daily IL2 treatments (day 4–10 and day 19–22, respectively). Kruskal-Wallis ANOVA on ranks: p < 0.01; post hoc Student-Newman-Keuls test: ^p < 0.05, ^^p < 0.01, ^^^p < 0.001, between the corresponding NTG+saline and NTG+IL2 groups; Friedman test: p < 0.001 within the NTG+saline group, ###p < 0.001, compared with the baseline threshold (day 1); p < 0.001 within the NTG+IL2 group, §p < 0.05, §§p < 0.01, §§§p < 0.001, compared with the baseline threshold (day 1).

(E) The slope of ld-IL2-induced reversal of mechanical threshold (same mice as in **D**). **p < 0.01, two-tailed t-test. The thresholds between day 5–11 and day 19–23 in individual mice were fitted by linear regression to calculate the slope, respectively.
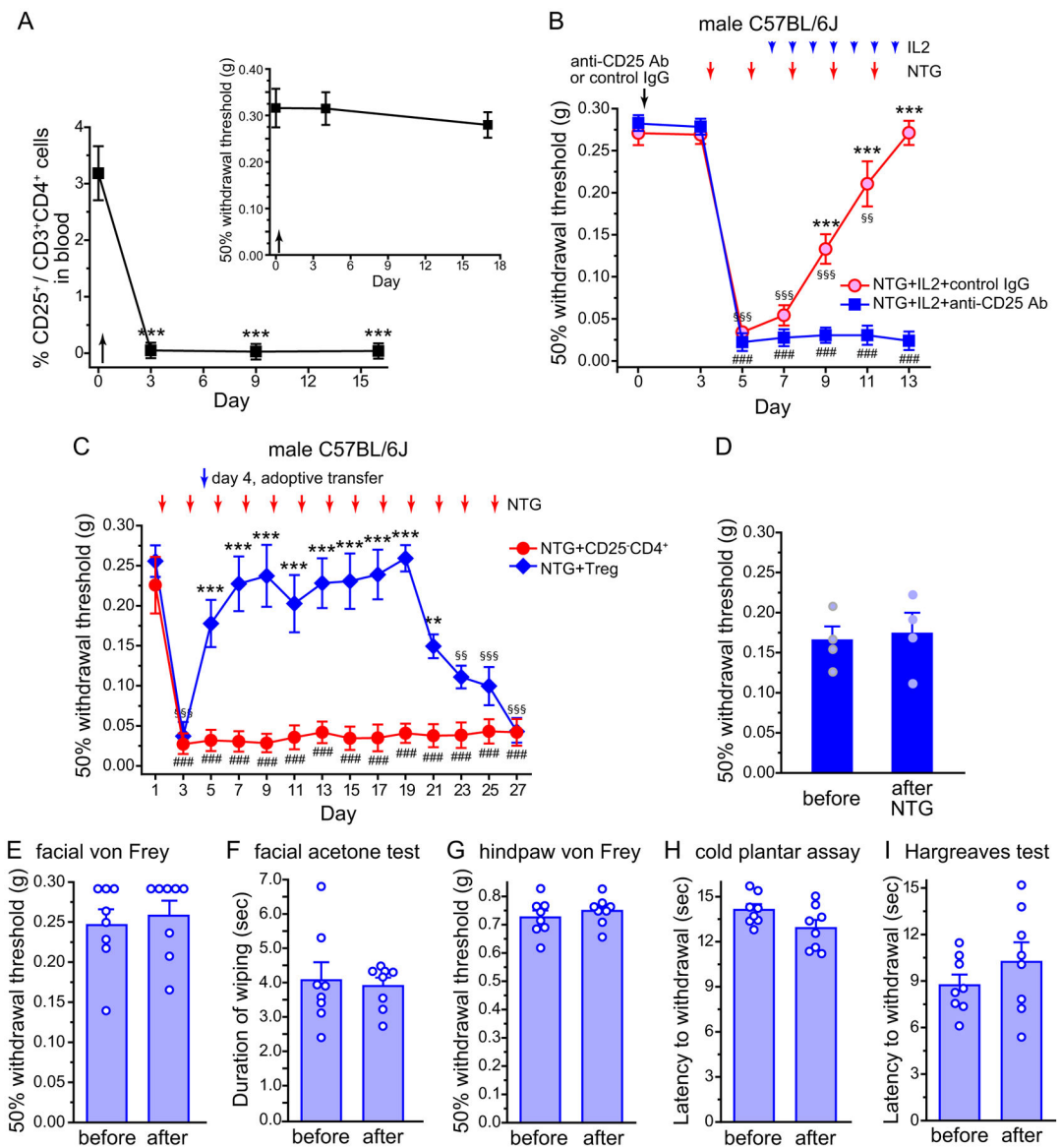
Figure 7. Treg cells mediate the therapeutic effect of ld-IL2.

(**A**) The frequency of $CD25^+$ Treg cells among $CD4^+CD3^+$ T cells in the peripheral blood of mice that received CD25 antibody on day 0 as indicated by the arrow (n = 4). One-way RM ANOVA with post hoc Bonferroni test: ***$p < 0.001$, compared with the baseline value (day 0). Inset: Depletion of Treg cells did not alter baseline facial mechanical thresholds.

(**B**) Depletion of Treg cells abolished the effect of ld-IL2. Male C57BL/6J mice received 1 i.p. injection of anti-CD25 antibody (Ab) or control IgG (n = 5 and 7, respectively). Three days later, mice were treated with NTG and IL2 injections as indicated by the arrows. Kruskal-Wallis ANOVA on ranks: $p < 0.01$; post hoc Student-Newman-Keuls test: ***$p < 0.001$, between the corresponding NTG+IL2+control IgG and NTG+IL2+anti-CD25 Ab groups; Friedman test: $p < 0.01$ within the NTG+IL2+anti-CD25 Ab group, ###$p < 0.001$, compared with the baseline threshold (day 3); $p < 0.001$ within the NTG+IL2+control IgG group, §§$p < 0.01$, §§§$p < 0.001$, compared with the baseline threshold.

(C) NTG-induced persistent facial skin hyper-sensitivity was reversed by the adoptive transfer of Treg cells. Male C57BL/6J mice received NTG injections every two days as indicated by the red arrows. On day 4, mice received adoptive transfer of Treg cells or CD25⁻CD4⁺ cells as indicated by the arrowhead (n = 6 per group). Kruskal-Wallis ANOVA on ranks: $p < 0.01$; post hoc Student-Newman-Keuls test: $**p < 0.01$, $***p < 0.001$, between the corresponding NTG+Treg and NTG+CD25⁻CD4⁺ groups; Friedman test: $p < 0.05$ within the NTG+CD25⁻CD4⁺ group, $^{\#\#\#}p < 0.001$, compared with the baseline threshold (day 1); $p < 0.05$ within the NTG+Treg group, $^{\S\S}p < 0.01$, $^{\S\S\S}p < 0.001$, compared with the baseline threshold.

(D) In 4 mice (out of the 6 mice in **C** NTG+Treg group), facial mechanical thresholds before and 3 hours after NTG injections were measured 1 week after the Treg adoptive transfer (day 11).

(E-I) Baseline nociception is not altered by Treg adoptive transfer. Baseline nociceptive responses were measured before and 6–10 days after the adoptive transfer of 1×10^6 Treg cells (n = 8 male C57BL/6J mice). **(E)** The 50% withdrawal thresholds to von Frey filaments on facial skin. **(F)** Time spent wiping the treated area after application of 12 μl acetone to the shaved cheek. **(G)** The 50% withdrawal threshold to von Frey filaments on the hindpaw. **(H)** The withdrawal latency to cold stimuli on the hindpaw. **(I)** The withdrawal latency to radiant heat stimuli on the hindpaw.
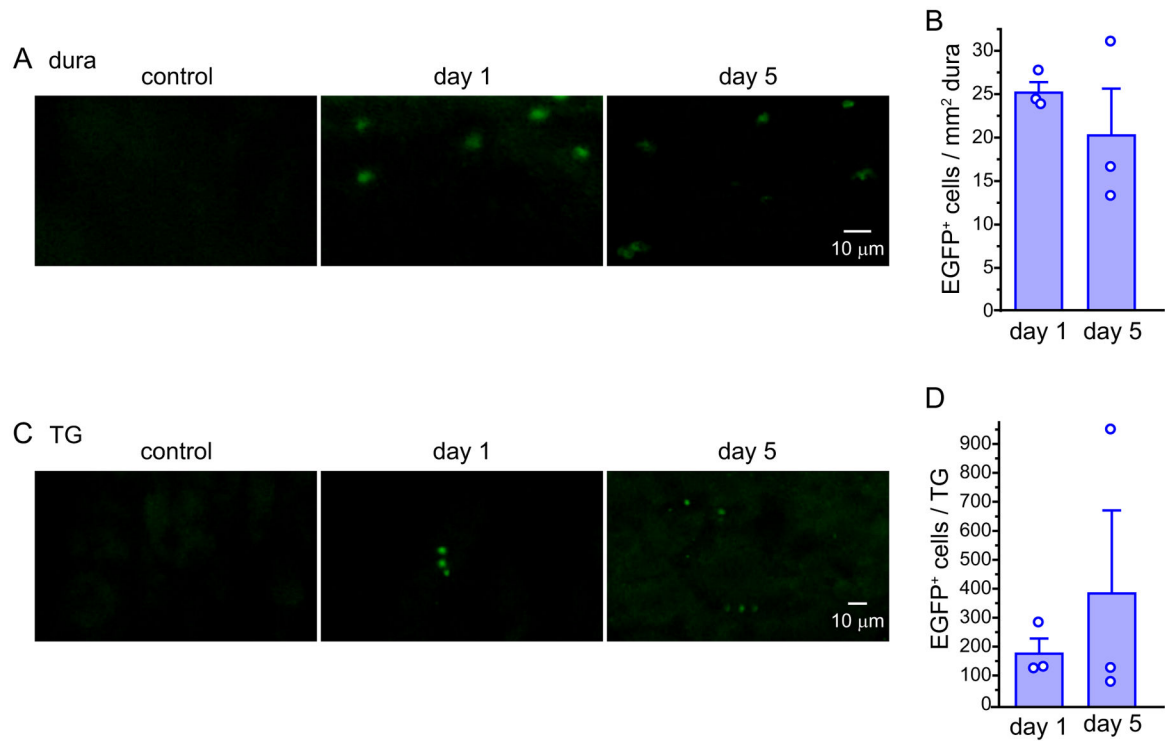
Figure 8. Adoptively transferred Treg cells traffic to the dura and TG.

(**A**) Representative images of EGFP+ Treg cells in the dura of a C57BL6/J mouse that received adoptive transfer of Treg cells from DEREG mice. The control image was from the dura of a naïve mouse.

(**B**) The number of EGFP+ Treg cells in the dura 1 and 5 days after adoptive transfer of Treg cells from DEREG mice to male C57BL6/J mice (n = 3).

(**C**) Representative images of EGFP+ Treg cells in TG sections from a C57BL6/J mouse that received adoptive transfer of Treg cells from DEREG mice. The control image was from the TG section of a naïve mouse.

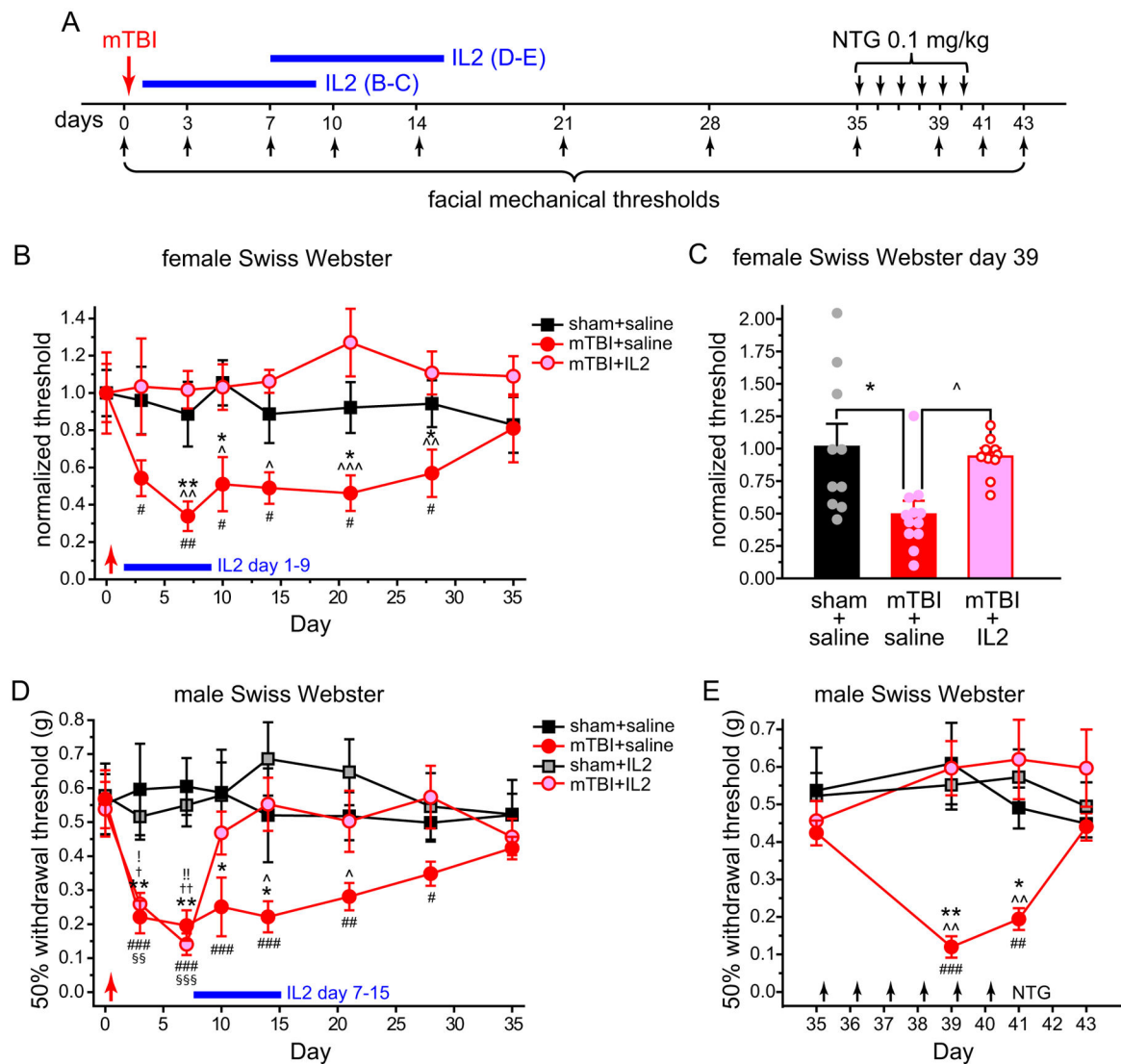(**D**) The number of EGFP+ Treg cells per TG 1 and 5 days after adoptive transfer (same mice as in **B**).

Figure 9. Ld-IL2 treatment reverses the facial skin hyper-sensitivity in a mouse model of mTBI-induced acute and persistent PTH.

(A) Time line of experiments. Note that IL2 and NTG were always injected after the completion of behavioral tests on the same day.

(B) mTBI-induced facial skin hyper-sensitivity in female Swiss Webster mice was prevented by ld-IL2 treatment between post-mTBI day 1–9 (n = 10–12 mice/group). The facial mechanical thresholds were normalized to the mean baseline values of individual groups on day 0 (before sham/mTBI). The arrow and the horizontal bar indicate the sham/mTBI procedure and the daily ld-I2 treatment, respectively. Kruskal-Wallis ANOVA on ranks: p < 0.01; post hoc Student-Newman-Keuls test: *p < 0.05, **p < 0.01, between the corresponding sham+saline and mTBI+saline groups; ^p < 0.05, ^^p < 0.01, ^^^p < 0.001, between the corresponding mTBI+saline and mTBI+IL2 groups; Friedman test: p < 0.05 within the mTBI+saline group, #p < 0.05, ##p < 0.01, compared with the baseline threshold (day 0).

(C) Normalized facial mechanical thresholds on day 39. Female Swiss Webster mice received 4 daily low-dose NTG injections (day 35–38) after the resolution of mTBI-induced facial skin hyper-sensitivity (same mice as in **B**). The facial mechanical thresholds were normalized to the mean values of individual groups on day 35 (before NTG injections). Kruskal-Wallis ANOVA on ranks: $p < 0.01$; post hoc Student-Newman-Keuls test: $*p < 0.05$ between sham+saline and mTBI+saline groups; $^\wedge p < 0.05$ between mTBI+saline and mTBI +IL2 groups.

(D) Delayed ld-IL2 treatment reversed mTBI-induced facial skin hyper-sensitivity in male Swiss Webster mice (n = 10–12 mice/group). The arrow and the horizontal bar indicate the sham/mTBI procedure and the daily ld-I2 treatment, respectively. Kruskal-Wallis ANOVA on ranks: $p < 0.05$; post hoc Student-Newman-Keuls test: $*p < 0.05$, $**p < 0.01$, between the corresponding sham+saline and mTBI+saline groups; $^\wedge p < 0.05$, between the corresponding mTBI+saline and mTBI+IL2 groups; $^\dagger p < 0.05$, $^{\dagger\dagger} p < 0.01$, between the corresponding sham +saline/IL2 and mTBI+IL2 groups; $^! p < 0.05$, $^{!!} p < 0.01$, between the corresponding sham +IL2 and mTBI+saline groups; Friedman test: $p < 0.001$ within the mTBI+saline group, $^\# p < 0.05$, $^{\#\#} p < 0.01$, $^{\#\#\#} p < 0.001$, compared with the baseline threshold (day 0); Friedman test: $p < 0.001$ within the mTBI+IL2 group, $^{\S\S} p < 0.01$, $^{\S\S\S} p < 0.001$, compared with the baseline threshold (day 0).

(E) After the resolution of mTBI-induced facial skin hyper-sensitivity, daily low-dose NTG injections produced persistent facial skin sensitization in mice that received mTBI but not in mice that received ld-IL2 treatment post-mTBI (same mice as in **D**). Arrows indicate NTG injections. Kruskal-Wallis ANOVA on ranks: $p < 0.001$; post hoc Student-Newman-Keuls test: $*p < 0.05$, $**p < 0.01$, between the corresponding sham+saline and mTBI+saline groups; $^{\wedge\wedge} p < 0.01$, between the corresponding mTBI+saline and mTBI+IL2 groups; Friedman test: $p < 0.001$ within the mTBI+saline group, $^{\#\#\#} p < 0.01$, $^{\#\#\#} p < 0.001$, compared with the pre-NTG threshold (day 35).
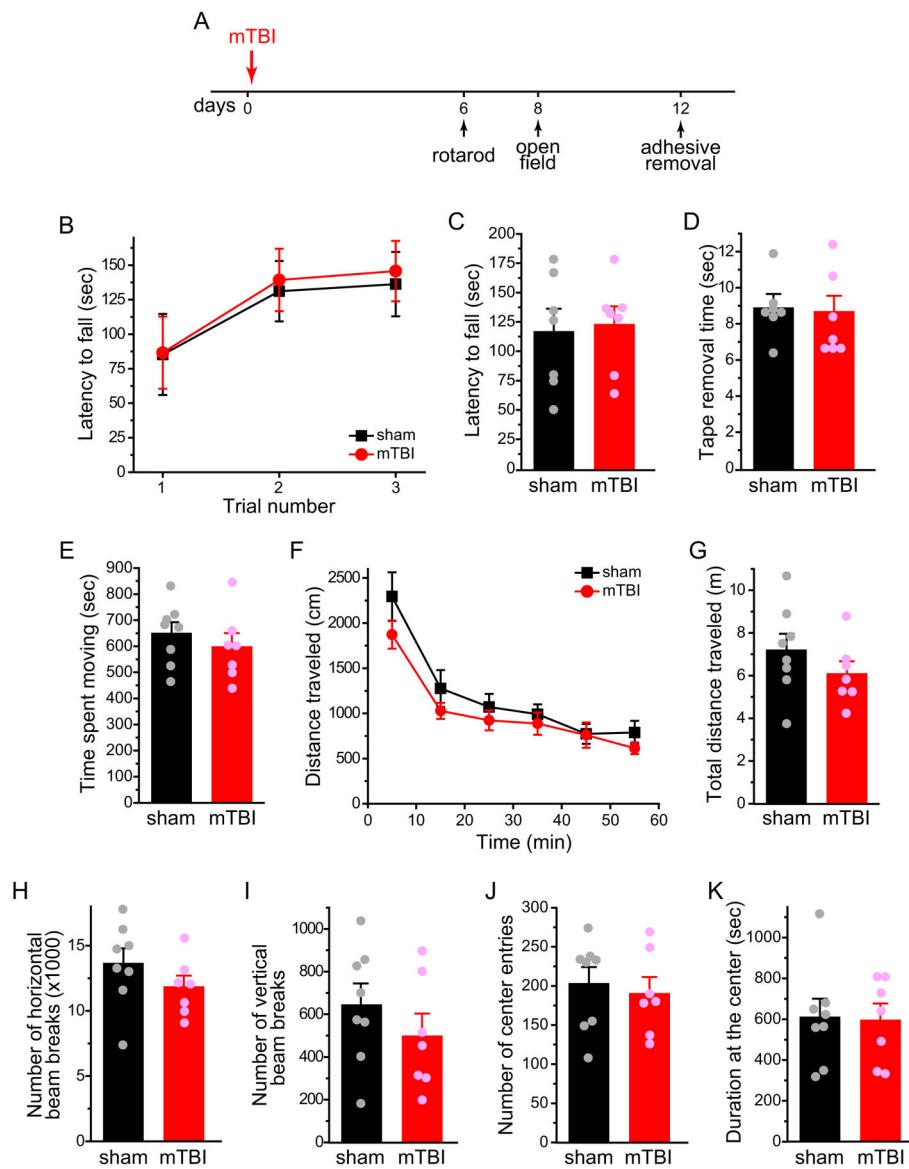
Figure 10. mTBI does not cause motor impairment.

(A) Time line of experiments.

(B) Latency to fall from the accelerating rotarod in 3 consecutive trials (n = 7 male Swiss Webster mice / group).

(C) The latency to fall from the accelerating rotarod was averaged from the 3 trials in individual mice (same mice as in **B**).

(D) The average time to remove adhesive tape strips was comparable between sham and mTBI mice (same mice as in **B**).

(E) Total time spent moving in the open field test (n = 8 and 7 male Swiss Webster mice in sham and mTBI groups, respectively).

(F) Distance traveled in the open field in 10-min bins (same mice as in **E**).

(G-K) Total distance traveled (**G**), the number of horizontal (**H**) and vertical (**I**) beam breaks, total number of entries into the center square (**J**) and total time spent in the center

square (**K**) during the 1-h testing period (same mice as in **E**). The results in **E-K** were confirmed with a second cohort of male Swiss Webster mice.
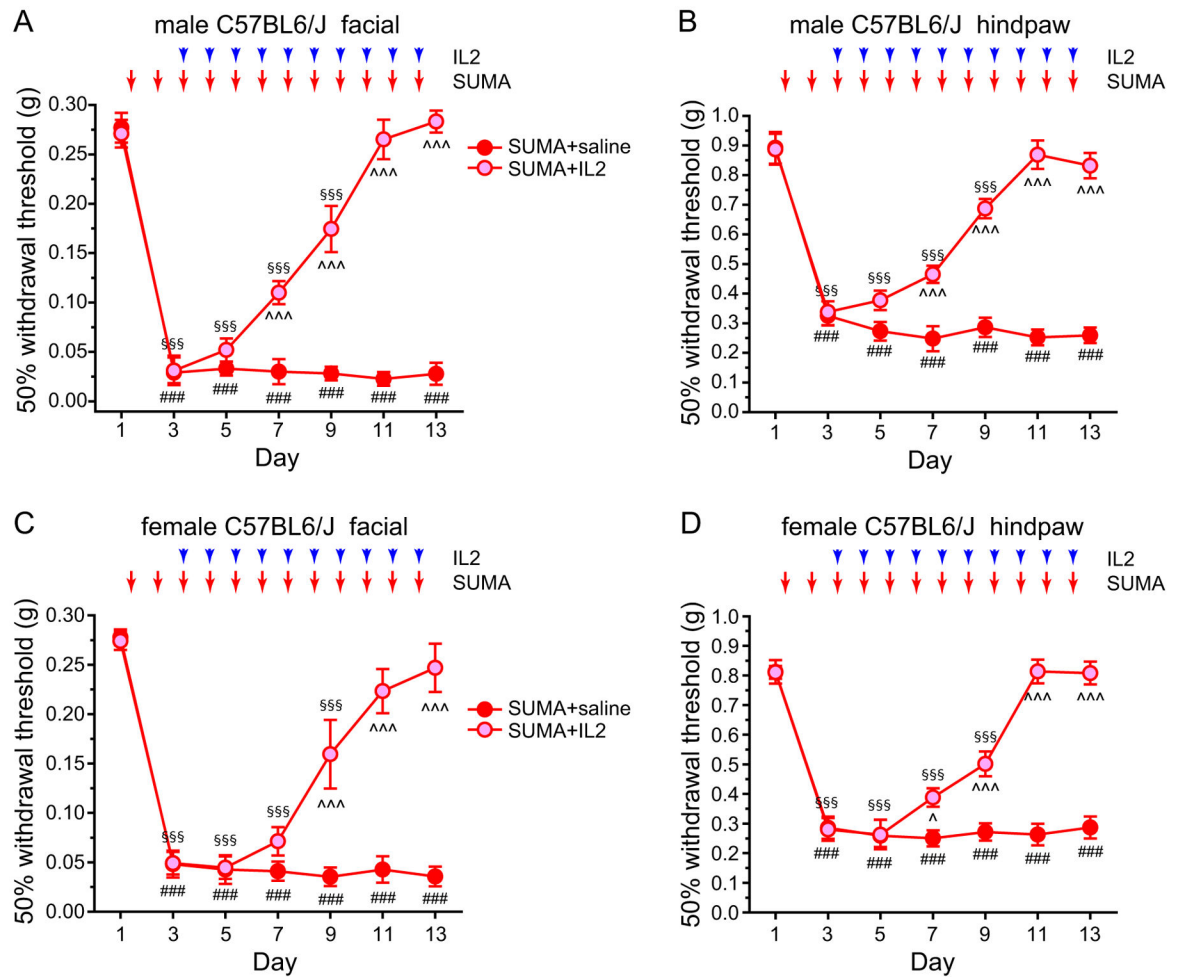
Figure 11. Ld-IL2 treatment reverses the skin hyper-sensitivity in a mouse model of MOH.
(A) Ld-IL2 treatment reverses the facial skin hyper-sensitivity induced by repeated administration of sumatriptan (SUMA) in male C57BL/6J mice (n = 6 and 7 mice in SUMA +saline and SUMA+IL2 groups, respectively). Arrows and arrowheads indicate the injections of SUMA and IL2, respectively. Note that IL2 and SUMA were always injected after the completion of behavioral tests on the same day. Kruskal-Wallis ANOVA on ranks: p < 0.01; post hoc Student-Newman-Keuls test: ^^^p < 0.001, between the corresponding SUMA+saline and SUMA+IL2 groups; Friedman test: p < 0.05 within the SUMA+saline group, ###p < 0.001, compared with the baseline threshold (day 1); p < 0.001 within the SUMA+IL2 group, §§§p < 0.001, compared with the baseline threshold (day 1).
(B) Repeated SUMA-induced hindpaw mechanical hyper-sensitivity is also reversed by ld-IL2 treatment (same mice as in **A**). Kruskal-Wallis ANOVA on ranks: p < 0.01; post hoc Student-Newman-Keuls test: ^^^p < 0.001, between the corresponding SUMA+saline and SUMA+IL2 groups; Friedman test: p < 0.001 within the SUMA+saline group, ###p < 0.001, compared with the baseline threshold (day 1); p < 0.001 within the SUMA+IL2 group, §§§p < 0.001, compared with the baseline threshold (day 1).
(C) Ld-IL2 reverses SUMA-induced facial skin hyper-sensitivity in female C57BL/6J mice (n = 5 and 8 mice in SUMA+saline and SUMA+IL2 groups, respectively). Kruskal-Wallis

ANOVA on ranks: p < 0.01; post hoc Student-Newman-Keuls test: ^^^p < 0.001, between the corresponding SUMA+saline and SUMA+IL2 groups; Friedman test: p < 0.05 within the SUMA+saline group, ###p < 0.001, compared with the baseline threshold (day 1); p < 0.001 within the SUMA+IL2 group, §§§p < 0.001, compared with the baseline threshold (day 1). **(D)** Repeated SUMA-induced hindpaw mechanical hyper-sensitivity is also reversed by ld-IL2 treatment in female mice (same mice as in **C**). Kruskal-Wallis ANOVA on ranks: p < 0.05; post hoc Student-Newman-Keuls test: ^p < 0.05, ^^^p < 0.001, between the corresponding SUMA+saline and SUMA+IL2 groups; Friedman test: p < 0.01 within the SUMA+saline group, ###p < 0.001, compared with the baseline threshold (day 1); p < 0.001 within the SUMA+IL2 group, §§§p < 0.001, compared with the baseline threshold (day 1).

Table 1.

Markers and assays used to define T cell subsets in this study

Markers	$CD3^+$	$CD3^+CD4^+$	$CD4^+CD25^+$	EGFP signal in DEREG mice	$CD3^+CD8^+$	IFNγ secretion assay
T cell subsets	total T cells	T helper cells	Treg cells [*]	Foxp3$^+$ Treg cells [**]	Cytotoxic T cells	Activation of T cells and other immune cells

[*] CD4$^+$CD25$^+$ cells from wild-type mouse splenocytes typically contain 70–93% Foxp3$^+$ cells.

[**] EGFP signal was present in 85–90% CD4$^+$CD25$^+$ splenocytes from adult DEREG mice.